

EXERGY REQUIREMENT AND EFFICIENCY OF BIOLOGICAL ACTIVITIES OF
CHLAMYDOMONAS REINHARDTII

by
Kübra Küçük

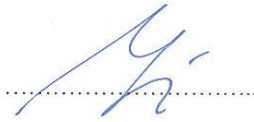
Submitted to the Institute of Graduate Studies in
Science and Engineering in partial fulfillment of
the requirements for the degree of
Master of Science in
Biotechnology

Yeditepe University
2014

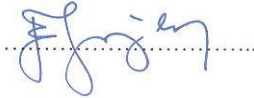
EXERGY REQUIREMENT AND EFFICIENCY OF BIOLOGICAL
ACTIVITIES OF *CHLAMYDOMONAS REINHARDTII*

APPROVED BY:

Prof. Dr. Mustafa Özilgen
(Supervisor)



Assoc. Prof. Dr. Esra Sorgüven Öner



Assist. Prof. Dr. Ali Özhan Aytekin



DATE OF APPROVAL:

ABSTRACT

EXERGY REQUIREMENT AND EFFICIENCY OF BIOLOGICAL ACTIVITIES OF *CHLAMYDOMONAS REINHARDTII*

Chlamydomonas reinhardtii is considered as a potential lipid producer for industrial biodiesel manufacture. The thermodynamic aspects of the lipid production process is important, since the non-lipid producing biological activities of the algal cultivation consume part of the solar energy captured with photosynthesis, in expense of the exergetic efficiency of the lipid production process. The cultivation of *Chlamydomonas reinhardtii* is modeled as a three-step chemical mechanism, which represents growth, respiration and lipid production and a thermodynamic analysis is performed. The results have indicated that the cumulative degrees of perfections of the biomass production processes are high when those of lipid production are low, and vice versa. The exergy destruction per unit biomass production are accountable under the favorable biological growth conditions, whereas the highest exergetic efficiency of the lipid production is accountable under the least favorable growth conditions, reconfirming the results of the previous studies that the lipid production takes place under the stress conditions.

Keywords: *Chlamydomonas reinhardtii*, photosynthesis, flagella work, lipid production, exergetic efficiency, cumulative degree of perfection

ÖZET

***CHLAMYDOMONAS REINHARDTII*'NİN BİYOLOJİK AKTİVİTELERİNİN EKSERJİ GEREKSİNİMİ VE VERİMLİLİĞİ**

Chlamydomonas reinhardtii, endüstriyel biyodizel üretimi için potansiyel bir lipit üreticisi olarak düşünülmektedir. Lipit üretim prosesinin termodinamik açısı algal kültürasyonunun lipit üretilmeyen biyolojik aktivitelerinin fotosentez ile ele geçirilen solar enerjinin bir kısmını tüketmesi ve lipit üretim prosesinin ekserjetik verimliliği açısından çok önemlidir. Bu çalışmada, *Chlamydomonas reinhardtii*'nin kültürasyonu büyümeyi, solunumu ve lipit üretimini temsil eden üç adımlı kimyasal bir mekanizma olarak modellendi ve termodinamik bir analiz yapıldı. Elde edilen sonuçlara göre, biyokütle üretimi prosesinin yetkinliğinin kümülatif derecesi lipit üretim prosesinininkine göre daha yüksek olduğu görüldü. Biyokütle üretimi başına ekserji yıkımının en yüksek görüldüğü biyolojik büyüme açısından yetersiz durumlarda, lipit üretiminin ekserjetik verimliliğinin en yüksek görülmesi, daha önceki çalışmalarda da düşünülen lipit üretiminin stres koşulları altında gerçekleşmesini tekrar onayladı.

Anahtar kelimeler: *Chlamydomonas reinhardtii*, fotosentez, kamçı işi, lipit üretimi, ekserjetik verimlilik, yetkinliğini kümülatif derecesi

TABLE OF CONTENTS

ABSTRACT.....	iii
ÖZET	iv
TABLE OF CONTENTS.....	v
LIST OF FIGURES	vii
LIST OF TABLES.....	viii
LIST OF SYMBOLS/ABBREVIATIONS.....	ix
1. INTRODUCTION	1
2. THERMODYNAMICS ON LIVING SYSTEMS.....	2
2.1. GIBB’S ENERGY CHANGE AND MICROBIAL GROWTH IN TERMS OF CATABOLISM AND ANABOLISM	5
2.2. MASS, ENERGY AND ENTROPY BALANCES	8
2.3. SYSTEMS FOR MICROBIAL GROWTH (OPEN-CLOSED SYSTEMS&ANEROBIC-ANAEROBIC MICROORGANISMS	12
3. BIOFUELS	14
3.1. THE ALGAE AND BIOFUELS	15
3.2. <i>CHLAMYDOMONAS REINHARDTII</i>	18
3.2.1. Studies on <i>Chlamydomonas Reinhardtii</i>	19
4. METHODS	21
4.1. EXPERIMENTAL DATA.....	22
4.2. MODELING CONSIDERATIONS	22
4.3. SYSTEM BOUNDARY	22
4.4. KINETIC ANALYSIS	23
4.5. THERMODYNAMIC ANALYSIS	24
4.6. WORK	25
4.7. PHOTON ENERGY	26
4.8. ESTIMATION OF THERMODYNAMIC PROPERTIES OF BIOCHEMICALS.....	26
4.9. OPTICAL EXERGY LOSS	28
4.10. CUMULATIVE DEGREE OF PERFECTION (CDP)	28

5. RESULTS	29
5.1. KINETIC MODEL	29
5.2. WORK	30
5.3. ENERGY LOSS	31
5.4. EXERGY DESTRUCTION	32
5.5. ECO-EXERGY	34
5.6. OPTICAL EXERGY LOSS	35
5.7. CUMULATIVE DEGREE OF PERFECTION (CDP)	36
6. CONCLUSION.....	39
REFERENCES	40
APPENDIX A.....	50
APPENDIX B	51
ALGORITHMS	53

LIST OF FIGURES

Figure 2.1. Biosynthesis and Gibbs energy dissipation in cellular growth.....	3
Figure 2.2. Breakdown of the Gibbs energy change per amount of biomass grown, $\Delta_r G_X$, into enthalpic and entropic components	4
Figure 2.3. The spontaneous transformation process occurring during cellular growth	5
Figure 2.4. Energy yielding and biosynthetic reactions.....	6
Figure 2.5. Energy yielding catalyzed by live cells	7
Figure 2.6. Entropy balance for a growing cell	9
Figure 2.7. Gibbs energy balance for a growing cell.....	10
Figure 3.1. Light microscopic photograph of <i>C. reinhardtii</i>	18
Figure 4.1. System boundary	23
Figure 5.1. Simulation of kinetic model of <i>Chlamydomonas reinhardtii</i>	30
Figure 5.2. Simulation of flagellar work of <i>Chlamydomonas reinhardtii</i>	31
Figure 5.3. Simulation of energy loss of <i>Chlamydomonas reinhardtii</i>	32
Figure 5.4. Concept of exergy in relation with our use in the given system	33
Figure 5.5. Simulation of exergy destruction of <i>Chlamydomonas reinhardtii</i>	34
Figure 5.6. Simulation of eco-exergy of <i>Chlamydomonas reinhardtii</i>	35

Figure 5.7. Simulation of optical exergy loss of *Chlamydomonas reinhardtii*..... 36

Figure 5.8. Simulation of CDP of *Chlamydomonas reinhardtii*..... 38

LIST OF TABLES

Table 3.1. Comparison of Fuels.....	14
Table A.1. Molecular weight and thermodynamical data of the compounds.....	50
Table B.1. Parameters of the kinetic models.....	51
Table B.2. Standard errors of estimate of the kinetic models.....	51
Table B.3. Summary of the thermodynamic assessment.....	52

LIST OF SYMBOLS/ABBREVIATIONS

A	Biomass concentration
b	Exergy
b_{ch}	Chemical exergy
F_d	Drag force
h	Enthalpy
R	Gas constant
T	Temperature
ΔG	Gibbs energy change
ΔG_b	Gibbs energy change of biomass
ΔG°	Standard molar Gibbs energy
\dot{S}_{prod}	Flux of entropy generated
ΔS	Entropy change
$Y_{X/S}$	Biomass yield
W	Work
0	Dead state
o	Initial state
ψ	Flux ratio
η	Efficiency
DCW	Dry cell weight

1. INTRODUCTION

Lipids are perfect chemicals to store internal energy in their interatomic high-energy bonds for future use. These high energy bonds serve as the energy reserve for organisms [1, 2] as well as for engines in form of biodiesel [3, 4]. *Chlamydomonas reinhardtii* is a unicellular photosynthetic, eukaryotic alga with a single chloroplast; it is widely used as a model system for the study of the photosynthetic processes [5]. The use of the photosynthetic algae as the source of raw material in biodiesel production may also stop the use of the foods with the same purpose in biofuel production [3]. Microalgae appear to be the only source of renewable biodiesel that is capable of meeting the global demand for transport fuels [3]. Algae-based biofuels are comprehensive and difficult to be categorized [6]. In the last few decades, numerous studies are published on exergy (availability) analysis [7-11]. Especially in the assessment of renewable energy sources, where we need to weigh various processes and fuels with respect to their ability to produce useful work and to identify their impact on the environment, exergy analysis provide a fair tool for comparison. In the last decade, numerous studies are published regarding the exergy analysis of the biological systems [4, 12-17], especially for the assessment of the efficiency of the exergy utilization via metabolic processes, and to relate kinetic parameters with thermodynamic functions [18, 19]. The aim of this study is to investigate exergy requirement and efficiency of biological activities of *C.reinhardtii*.

2. THERMODYNAMICS IN LIVING SYSTEMS

The thermodynamics of microbial growth involves a combination of sciences such as biology, chemistry and physics, and related to many ideas from these separate disciplines. Generation of some form of limiting boundary is required in order to separate a working growth-process system from its environment. As the system passes from a thermochemically defined initial state to a thermochemically defined final state, the energy changes can be determined instantaneously or as the result of the consumption of a given quantity of substrate [20].

The laws of thermodynamics which all living organisms obey these laws form the basis all laws. Nature progresses become from more order to less order in isolated systems. The suggestion is that the term the passage of time does not exist, only entropy increases at the macro level, with living organisms capable of decreasing entropy at the level of living systems [21].

Due to the irreversible nature of life processes, the dissipation of Gibbs energy invariably and continuously reflects itself in a continuous release of heat.

Heat effects in cellular cultures are often not noticed while working with conventional laboratory equipment since most of the heat release by the culture is lost to the environment too quickly to cause a perceivable temperature increase. However, this is reverse for large scale. Industrial size fermenters operate nearly adiabatically due to small surface-to-volume ratio. Hence, all the heat released by the culture should be removed by proper cooling facilities. Thus, having sufficient quantitative information on microbial heat release is important while designing the cooling facilities for biotechnological processes.

Figure 2.1 is the illustration of the continuous heat generation for a growing cell culture. Living cell consists of biopolymers, membranes, functional structures organelles and all the other highly complex materials and the biosynthesis of these items from simple molecules such as carbohydrates and simple salts, is endergonic due to entropic reasons. In chemotrophic organisms, as the reactions taking place simultaneously, all the biosynthetic

reactions can be driven due to one or several catabolic or ‘energy-yielding’ reactions despite the increase of ΔG .

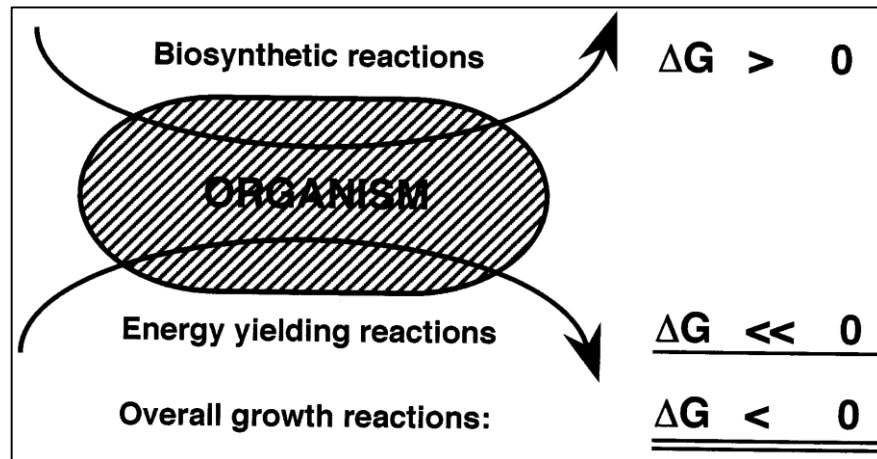


Figure 2.1. Biosynthesis and Gibbs energy dissipation in cellular growth [18]

ΔS of the energy yielding reaction is so large that growth proceeds despite an overall increase of enthalpy in fermentation process and the cultures in this process would be endothermic and hence cool their environment (far left of Figure 2.2). In Figure 2.2, arrows pointing downwards indicate a positive entropy change ΔS , thus contributing negatively to ΔG .

Furthermore, dissipation of free energy and growth yield are related as shown in Figure 2.1. The growth yield should be small, but both the heat generation and the Gibbs energy dissipation per amount of biomass will be substantial in order to drive the biosynthesis of a given amount of biomass, hence a large amount of free energy would be dissipated. On the other hand, there will only be a small heat effect, however the growth yield will be large if the metabolism gets away with only modest energy dissipation for the same growth. In an idealized growth process, which gives the upper limit of the growth yield, the free energy changes of the biosynthetic and the energy yielding reaction cancel each other so that the overall dissipation Gibbs energy becomes zero. However, real growth processes are far away from this limit.

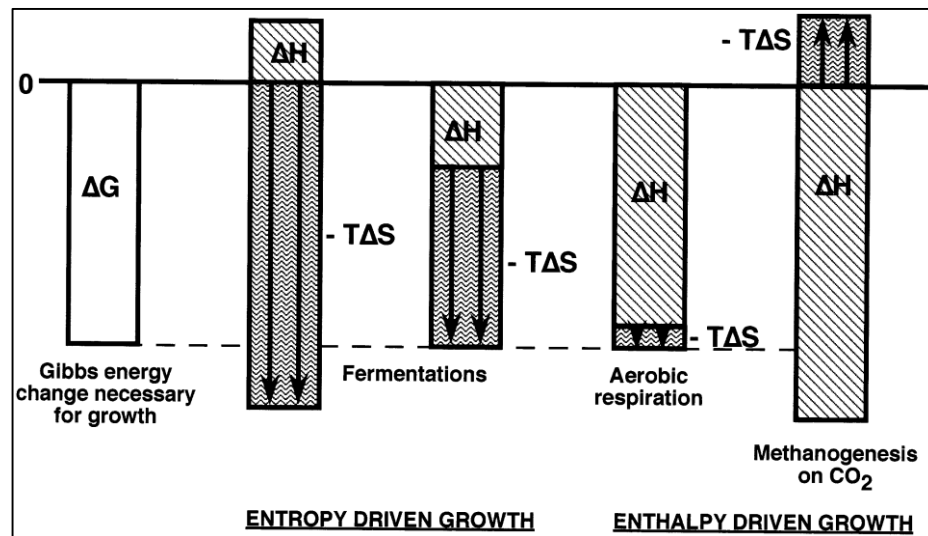


Figure 2.2. Breakdown of the Gibbs energy change per amount of biomass grown, $\Delta_r G_X$, into enthalpic and entropic components [18]

Due to the relation of free energy dissipation and growth mentioned above, a thermodynamic analysis offers to provide potential as a basis for predicting growth yields. Several correlations have been proposed comparing actual growth stoichiometry with the upper limit called thermodynamic efficiencies.

The most recent and complete of the correlations is by Heijnen and co-workers which is based on a wide range of literature survey and correlates the overall Gibbs energy dissipation as well as the maintenance requirements in terms of simple variables such as the number of carbon atoms and the degree of reduction of the carbon and energy source. These kinds of analyses are highly useful for predicting biomass yields and microbial stoichiometry based on a minimal amount of information due to black-box approach. On the other hand, yields of non-catabolic metabolites cannot be predicted well, nor indicate whether and how product yields could be improved. A more detailed analysis of the metabolism has to be performed for this [18].

2.1. GIBBS ENERGY CHANGE AND MICROBIAL GROWTH IN TERMS OF CATABOLISM AND ANABOLISM

The thermodynamic analysis of microbial growth consists of considering the latter as a spontaneous process transforming a number of reactants or substrates into products, one of which is the newly produced biomass (Figure 2.3).

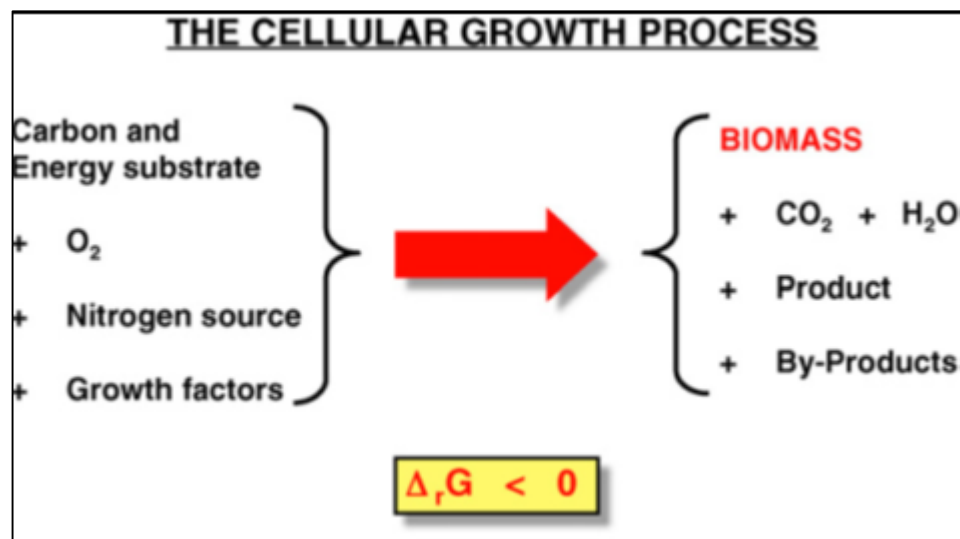


Figure 2.3. The spontaneous transformation process occurring during cellular growth [22]

According to classical thermodynamics, the Gibbs energy change related to this transformation process must be negative. However, it is not obvious why growth is so spontaneous and how ΔG can be negative because dry biomass may be expected to represent relatively high Gibbs energy form of matter. The reason is not that it contains an abnormally high internal energy; however it is a well-organized form of matter containing many polymers, which may therefore be characterized by relatively low entropy. The problem is usually analyzed by splitting the overall growth process as shown in Figure 2.3 into so-called anabolic and catabolic reactions (Figure 2.4).

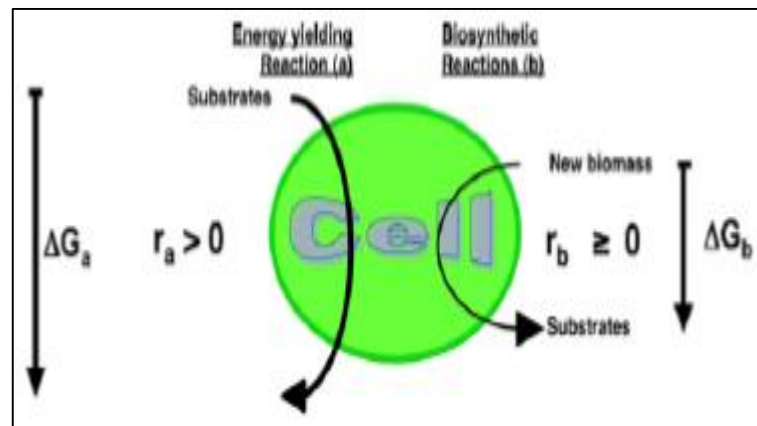


Figure 2.4. Energy yielding and biosynthetic reactions [22]

If these reactions were independent, they would both proceed downwards on a Gibbs energy scale and biomass would decay rather than being synthesized depending on the value of ΔG_b .

If the anabolic reactions in the cell, which result in the synthesis of the new biomass from chemical compounds acting as carbon, nitrogen and other sources, were independent from other processes, they would certainly not cause a strong decrease, but might rather result in an increase of Gibbs energy. Since biomass would be in a state of higher Gibbs energy than the growth substrates as it can be seen in reaction (b) in Figure 2.4., biomass could not be synthesized, but would rather have the tendency to decay into simpler molecules. In order to prevent this and to drive biomass synthesis “up-hill” against a positive Gibbs energy gradient, anabolic reactions are coupled in live cells by biochemical mechanisms to an energy yielding or catabolic reaction which is sufficiently exergonic to make the combination of the two reactions possible (Figure 2.5).

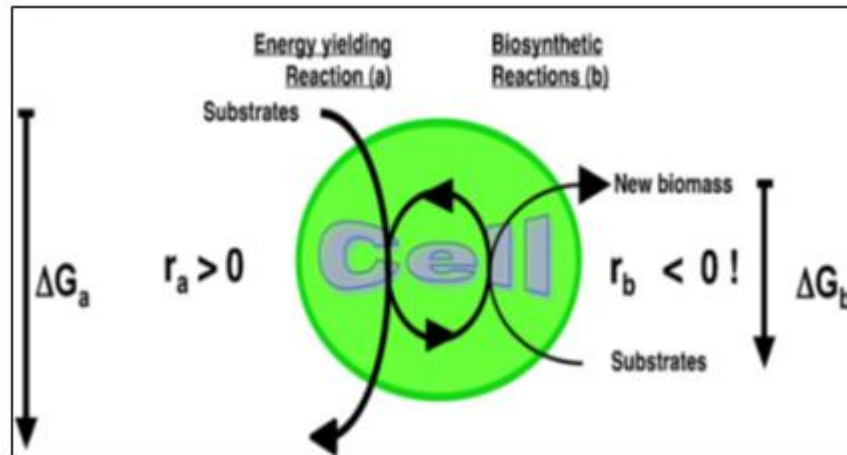


Figure 2.5. Energy yielding catalyzed by live cells [22]

Biochemical coupling between reactions (a) and (b) in Figure 2.5 can drive reaction (b) “upwards” against Gibbs energy driving force.

Whether the resulting overall change of Gibbs energy for this combination is really negative and by which amount is determined by the relative rates of the “driving” catabolic reaction (r_a) and the “payload” anabolic reaction (r_b in Figure 2.5):

$$\Delta_r G^\circ = \Delta G_a^\circ + \psi \Delta G_b^\circ \quad (2.1)$$

where ψ is the flux ratio of reaction (b) to (a) defined by;

$$\psi = \frac{r_b}{r_a} \quad (2.2)$$

In these equations, r_a and r_b are the rates of reactions (a) and (b) in Figure 2.5, and ΔG_a° , ΔG_b° and $\Delta_r G^\circ$ denote the standard molar Gibbs energies of, respectively, reactions (a) in and (b) in Figure 2.5, and the standard Gibbs energy of the combined process expressed per mole of catabolized energy substrate. Standard Gibbs energies may be used in these equations since the Gibbs energy changes are so involved so that the concentration dependent terms may be neglected.

r_a and r_b are both positive in coupled systems. r_b runs “backwards” against a possible positive Gibbs energy gradient because of biochemical coupling of the two reactions and hence becomes negative, making Ψ negative. Thus, the second righthand term of Eq. (2.1) will make the overall change in Gibbs energy, $\Delta_r G^0$ less negative. As the flux ratio, Ψ becomes larger, this effect will be more evident. The flux ratio, Ψ is translated into a bioenergetic growth efficiency which is a well-known method to visualize the effect of itself.

Many different bioenergetic efficiencies have been defined, however many of these simplified to a so-called energy transducer efficiency characterizing the fraction of the Gibbs energy released by the driving reaction (a) which can be recovered in the form of Gibbs energy stored in the newly grown biomass:

$$\eta = -\frac{\psi \Delta G_b^0}{\Delta G_a^0} \quad (2.3)$$

Equation (2.4) is obtained by combining Eqs. (2.3) and (2.1);

$$\Delta G_r^0 = \Delta G_a^0 (1 - \eta) \quad (2.4)$$

which implies that the overall change of Gibbs energy is proportional to the energetic inefficiency, that is the fraction of the energy dissipated and hence lost. If Gibbs energy loss or the bioenergetic growth efficiency η can be predicted and the relationship between Ψ and $Y_{X/S}$ is known, the biomass yield $Y_{X/S}$ may be predicted from Eqs. (2.1) or (2.3) [22].

2.2. MASS, ENERGY AND ENTROPY BALANCES

Microbial growth occurs spontaneously and is evidently a highly irreversible phenomenon. Hence, it must be coupled with the production of entropy. Due to growth reactions this is contradictory, since growth reactions produce matter in a highly organized form from a set of very simple small molecules. One intuitively thinks that microbial growth decreases the entropy instead of producing it.

This contradiction may be overcome by contemplating an open-system entropy balance for the growing microbial cell (Figure 2.6);

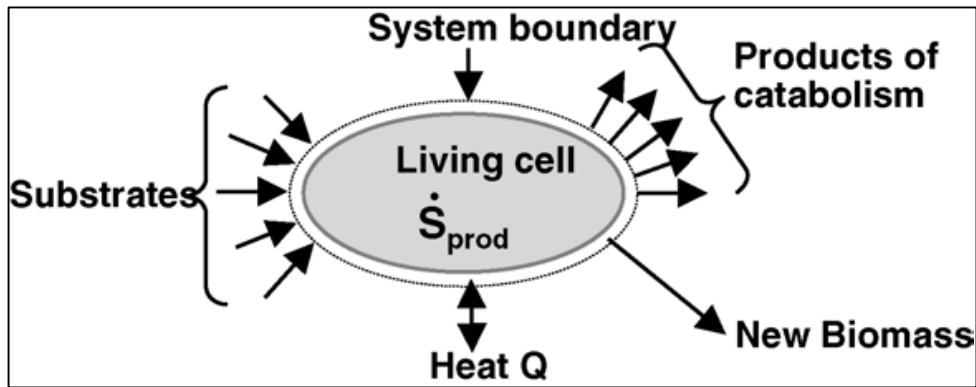


Figure 2.6. Entropy balance for a growing cell [23]

In Figure 2.6, \dot{S}_{prod} represents the flux of entropy generated inside the cell due to irreversible processes.

$$\frac{dS}{dt} = \frac{\dot{Q}}{T} + \sum_i \bar{s}_i \dot{n}_i - \bar{s}_X \dot{n}_X + \dot{S}_{\text{prod}} \quad (2.5)$$

According to Equation (2.5), the entropy change in the cell with time is given by the sum of all entropy fluxes exchanged with the environment plus the entropy production rate by irreversible processes (\dot{S}_{prod}). Entropy may be exchanged with the environment due to heat transfer to or from the cell denoted by \dot{Q}/T (dQ_{rev}/T represents the entropy increase in closed systems). In open systems, entropy is also imported or exported through metabolites entering or leaving the cell where \bar{s}_i denotes the partial molar entropy carried by the i^{th} metabolite and \dot{n}_i its molar rate of exchange and positive values indicate assimilation rates. Newly formed biomass is considered as a product of the cell leaving at a C-molar rate of \dot{n}_X . Its partial molar entropy \bar{s}_X is low due to the high degree of organization of matter. The entropy production rate by irreversible processes \dot{S}_{prod} can only be positive according to the Second Law of Thermodynamics and it represents the real driving force for the process.

Due to constant entropy production at rate \dot{S}_{prod} and due to the fact that newly formed cells of low entropy content leave the cell but have been synthesized by importing high-entropy metabolites, entropy could accumulate in the cell in principle, and cause thermal cell death or to structural disorganization. In order to avoid this, the cell must constantly export the excess entropy, which means keeping dS/dt at zero by making the sum of the first three terms on the right-hand side of Eq. (2.5) negative due to the precise role of catabolism. It exports the excess entropy either by creating a large flux of small waste molecules from the substrate, therefore exporting it in the form of chemical entropy and making $\sum_i \bar{s}_i \cdot \dot{n}_i - \bar{s}_X$ negative, or by releasing considerable amounts of heat, and hence making \dot{Q}/T also negative. If Eq. (2.5) is multiplied by T and subtracted from an enthalpy balance which is Eq. 2.6 for a constant pressure process

$$\frac{dH}{dt} = \dot{Q} + \dot{W} + \sum_i \bar{h}_i \cdot \dot{n}_i - \bar{h}_X \cdot \dot{n}_X \quad (2.6)$$

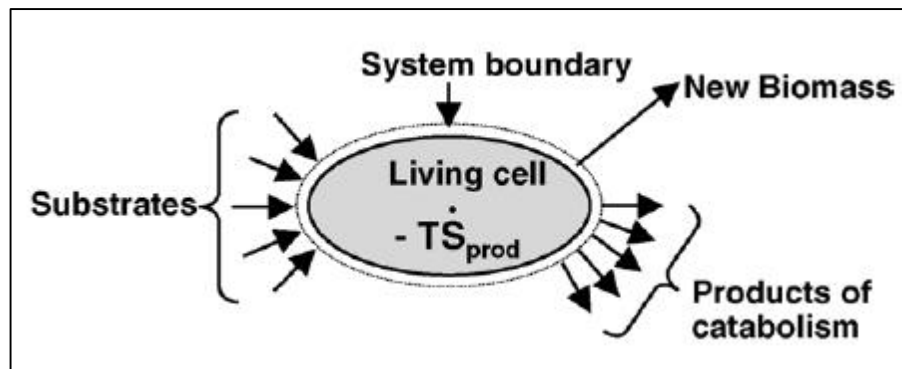


Figure 2.7. Gibbs energy balance for a growing cell [23]

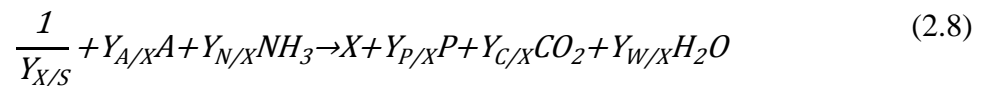
A Gibbs energy balance results (Figure 1.7);

$$\frac{dG}{dt} = \dot{W} + \sum_i \mu_i \cdot \dot{n}_i - \mu_X \cdot \dot{n}_X - T \dot{S}_{prod} \quad (2.7)$$

where \dot{W} stands for the power or work done on the cells, and μ_i and μ_X stand for the chemical potential of the i th metabolite and the newly grown cells, respectively. The latter

is high due to the low entropy of biomass. In order to avoid death, the cell has to keep dG/dt at zero despite a constant loss of Gibbs energy through the newly formed biomass ($-\mu_X \cdot \dot{n}_X$) and through dissipation or destruction of Gibbs energy ($-T\dot{S}_{prod}$), that can only be negative. In phototrophs, this loss is settled by a positive \dot{W} term in the form of photons. On the other hand, chemotrophs have a catabolism that feeds on high Gibbs energy substrates and release low energy waste products, thus making $\sum_i \mu_i \cdot \dot{n}_i$ positive so that it overcompensates $-\mu_X \cdot \dot{n}_X$ and $-T\dot{S}_{prod}$. Gibbs energy continuously decreases in the surrounding medium as a result.

The change in Gibbs energy in terms of Gibbs energy of reaction, ΔG can be expressed by writing the whole process in form of a macrochemical equation, of which an example for chemotrophic growth could have form of Equation (2.8) below;



where S , A , X and P represent the carbon source, an electron acceptor or donor, the newly grown biomass, and a catabolic waste product, respectively. $Y_{X/S}$ denotes the yield of biomass on the carbon source and $Y_{i/X}$ denotes the other yields. All Y coefficients may be considered as stoichiometric coefficients of the growth reaction.

A molar balance over the cells for any of the metabolites in a macrochemical equation such as Equation (2.8) yields;

$$\frac{dn_i}{dt} = \dot{n}_i + v_i \cdot \dot{\xi} \quad (2.9)$$

where v_i stands for either $1/Y_{X/S}$ or any of the other Y_i/X and $\dot{\xi}$ denotes the rate of the growth reaction in C mol s^{-1} per one cell. Then, Equation (2.10) is obtained by substituting Equation (2.9) into Equation (2.7) and assuming the cells to be at steady state, which means both dG/dt and dn_i/dt are taken as zero [19];

$$\Delta_r G_X \dot{\xi} = \dot{W} - T \dot{S}_{prod} \quad (2.10)$$

with

$$\Delta_r G_X \equiv \sum_i \nu_i \mu_i = \Delta_r H_X - T \Delta_r S_X \quad (2.11)$$

where $\Delta_r G_X$ denotes the molar Gibbs reaction energy of the macrochemical reaction. The sum in Eq. (2.11) has to be performed over all constituents of the macrochemical Eq. (2.8) including biomass.

\dot{W} is usually zero in non-photosynthetic growth. In this case, Eq. (2.10) shows that $\Delta_r G_X \dot{\xi}$ reflects the rate at which cells export the entropy produced by irreversible processes into the fermentation medium. $\Delta_r G_X$ must obviously be negative for growth to occur since \dot{S}_{prod} can only be positive. Thus, $\Delta_r G_X \dot{\xi}$ also reflects the rate at which Gibbs energy is dissipated by irreversible processes occurring in the cells. Therefore, the Gibbs energy in the growth medium will decrease at a corresponding rate.

Due to the direct relationship with the rate of entropy generation in the case of $\dot{W} = 0$ (Eq. (2.10)), $\Delta_r G_X$ is the driving force for its conjugate flux $\dot{\xi}$. As shown in Eq. (2.11), the driving force has an enthalpic and an entropic part, which is related to the export of entropy in the form of heat and in the form of high entropy molecules, respectively [22].

2.3. SYSTEMS FOR MICROBIAL GROWTH (OPEN-CLOSED SYSTEMS & AEROBIC-ANAEROBIC MICROORGANISMS)

Initially, systems involving the lowest number of reactants and products must be used, and this involves the use of microorganisms for such a study. Individual microbial cells are open systems, and it is not practical to study individually. It is easier to deal with the aggregate as products of a growth process. Open systems in the form of continuous cultures can be used. However, because of their method of working, continuous cultures are usually rate-limited, and may (or may not) accumulate storage substances that are not a part of the fabric of the cells. This may increase obviously the apparent cellular yield on a given substrate. Closed systems offer many advantages. The limiting boundary can be the wall of a closed batch culture vessel which contains a thermochemically defined culture

medium that constitutes the initial state of a growth-process system. There must be adequate head space above the culture medium to allow gas exchange. For aerobic cultures, the initial state must contain $O_2(aq)$ which is supplied by $O_2(g)$ in the head space. For anaerobic cultures, the head space is filled with an inert gas. Due to the utilization of a small amount of substrate, the amount of PV work done by any change in gas pressure is minimal, and usually be neglected relative to the total energy changes taking place. A few cells must be inoculated into the medium; however the mass of the cells is so small that this can be neglected as a part of the initial state. The cells act as self-reproducing catalysts during the process of growth, and their number increases in order to become the mass of one of the products of the final state existing after the substrate has been completely consumed. The other products of the final state usually contain $CO_2(aq)$, $H_2O(l)$, and any organic products other than the cells. These latter are always generated during fermentative growth processes. A growth-process equation that satisfies the Law of the Conservation of Mass can be used to represent the initial and final states. Then, the aim is to determine the energy changes which occur during the process of growth as this passes from an initial to a final state in a closed system, in a manner that satisfies the Law of the Conservation of Energy. Theoretically, any microorganism can be used as a biological tool for thermodynamic studies, if it can be grown on a single substrate and that thermochemically definable products are formed during the growth process [20].

3. BIOFUELS

Fuels are materials storing potential energy that can be released and used as heat energy. The energy of a biofuel is obtained through biological carbon fixation in which inorganic carbon is converted into organic compounds. If this process occurs in a living organism, it will be defined as 'biological carbon fixation'. The chemical structure of biofuels differs as the chemical structure of fossil fuels. Types biofuels with their fossil fuel counterparts are tabulated in Table 3.1. below [24].

Table 3.1. Comparison of Fuels [24]

Biofuel	Fossil Fuel	Differences
Ethanol	Gasoline/ethane	Ethanol has almost half the energy per mass of gasoline. Ethanol burns cleaner than gasoline, but produces less carbon monoxide. Ethanol produces more ozone than gasoline and contributes to smog. Engines must be modified to run on ethanol.
Biodiesel	Diesel	Biodiesel has slightly less energy than regular diesel. It is more corrosive to engine parts than standard diesel; engines have to be designed to take biodiesel. It burns cleaner than diesel, producing less particulate and fewer sulfur compounds.

Methanol	Methane	Methanol has about one third to one half as much energy as methane. Methanol is a liquid and easy to transport but methane is a gas that must be compressed for transportation.
Biobutanol	Gasoline/butane	Biobutanol has slightly less energy than gasoline, but can run in any car using gasoline without the need for modification to engine components.

Biofuels contribute little or no CO₂ to the buildup of greenhouse gas emissions. Converting biomass sources to biofuels is an environmentally friendly process as using biofuels for transportation. When biofuels are used [25]:

- the emissions associated with gasoline are avoided.
- the CO₂ content of the fossil fuels are allowed to remain in storage.
- mechanism for CO₂ absorption is provided by growing new biomass for fuels.

Biofuels offer the most beneficial alternative to reduce greenhouse gases from the transportation sector since they are compatible with the natural carbon cycle [25].

3.1. THE ALGAE AND BIOFUELS

The algae biofuels industry consists of many pathways in order to produce fuels from algae. This industry is developing rapidly and since there are thousands of different algal strains, abundance of cultivation and harvest methods, wide range of algae products, and host of technologies which are used to convert these products into different transportation fuels, algae-based biofuels are comprehensive and difficult to be categorized [6].

Algae are eukaryotic and carry out photosynthesis within membrane-bound organelles called chloroplasts. Chloroplasts contain circular DNA which is similar in structure to cyanobacteria. Algae are featured in bodies of water, common in terrestrial environments. They are classified into three groups based on their pigmentation: brown seaweed (*Phaeophyceae*), red seaweed (*Rhodophyceae*) and green seaweed (*Chlorophyceae*). Microalgae are unicellular photosynthetic microorganisms, living in saline or fresh water environments that convert sunlight, water and carbon dioxide to algal biomass. The three most important classes of microalgae in terms of abundance are the diatoms (*Bacillariophyceae*), the golden algae (*Chrysophyceae*) and the green algae (*Chlorophyceae*). Among the class of the green algae, *Chlorophyceae*, those most widely used belong to the genera *Chlamydomonas*, *Chlorella*, *Haematococcus*, and *Dunaliella*. Microalgae flourish in aerated, liquid cultures where the cells can access to light, carbon dioxide, and other nutrients necessary for maintenance. Algae are primarily grown photoautotrophically; nevertheless, some of are able to survive heterotrophically by degrading organic substances like sugars. Unlike terrestrial plants, microalgae do not require fertile land or irrigation. Since algae consume carbon dioxide, large-scale cultivation can be used to remediate the combustion exhaust of power plants. Algae biomass can play an important role in solving the problem between the production of food and that of biofuels in the near future. Microalgae appear to be the only source of renewable biodiesel that is capable of meeting the global demand for transport fuels [26]. The growth rate of algae and the oil content of the biomass determine the oil productivity. Microalgae with high oil productivities are preferred to be used for producing biodiesel [6].

Algae are sunlight-driven cells which can be used in bioremediation and as fertilizers for fixing nitrogen. Additionally, these photosynthetic microorganisms can transform carbon dioxide to potential foods and fuels. Microalgae can provide renewable biofuels in several different ways including photobiological biohydrogen production; methane production derived from anaerobic digestion of the algal biomass; and biodiesel produced from microalgal oil [6]. Hence they are attractive raw material for biofuels compared to other biofuel sources. It was claimed that algae biofuel yields that are theoretically orders of magnitude higher than other biofuels feedstock because of their rapid growth rate (doubling in 6–12 hours), high oil content (4–50% or greater of nonpolar lipids), biomass harvest (100%), and non-seasonal harvest intervals have led to claims of. On the other

hand, the diversity of algal characteristics and lack of scientific and industry consensus have made it difficult until nowadays to estimate the true potential of algae as a fuel source [27].

Many algal species have been found to grow rapidly and produce substantial amounts of triacylglycerol (TAG) or oil, and are hence called as oleaginous algae. Algae could be employed as cell factories to produce oils and other lipids for biofuels and other biomaterials. The potential advantages of algae as source for biofuels and biomaterials include [28]:

- i. synthesizing and accumulation large quantities of neutral lipids/oil (20–50% of dry cell weight (DCW)),
- ii. growth at high rates (e.g. 1–3 doublings per day),
- iii. thriving in saline/brackish water/coastal seawater for which there are few competing demands,
- iv. toleration of marginal lands (e.g. desert, arid- and semi-arid lands) that are not suitable for conventional agriculture,
- v. utilization growth nutrients such as nitrogen and phosphorus from a variety of wastewater sources (e.g. agricultural run-off, concentrated animal feed operations, and industrial and municipal wastewaters), providing the additional benefit of wastewater bio-remediation,
- vi. separation of carbon dioxide from flue gases emitted from fossil fuel-fired power plants and other sources, thereby reducing emissions of a major greenhouse gas,
- vii. production of value-added co-products or by-products (e.g. biopolymers, proteins, polysaccharides, pigments, animal feed, fertilizer and H₂),
- viii. growth in suitable culture vessels (photo-bioreactors) throughout the year with an annual biomass productivity, on an area basis, exceeding that of terrestrial plants by approximately tenfold.

3.2. *CHLAMYDOMONAS REINHARDTII*

Chlamydomonas reinhardtii is a unicellular eukaryotic alga possessing a single chloroplast that is widely used as a model system for the study of photosynthetic processes [5, 29].



Figure 3.1. Light microscopic photograph of *C. reinhardtii* [30]

C. reinhardtii is commonly found among soil and fresh water habitats and spends most of its life cycle as a haploid mitotic (vegetative) cell [29].

C. reinhardtii, biflagellate green alga in the order Volvocales, provides unique advantages to study eukaryotic flagella and basal bodies. It uses flagella for motility and for cell-cell recognition during mating. Flagella may be isolated easily for biochemical analysis since it is located on the surface of the cell. Despite *C. reinhardtii* and mammals are separated by more than 10^9 years of evolution, *C. reinhardtii* flagella are surprisingly similar in structure and function to mammalian cilia and flagella. For example, some of the flagellar proteins in *C. reinhardtii* are similar to proteins with similar function in human sperm more than 75% [31].

Synchronized cultures of the green alga *C. reinhardtii* are grown photoautotrophically under a wide range of environmental conditions such as temperature (15–37°C), different mean light intensities (132, 150, 264 $\mu\text{mol m}^{-2}\text{s}^{-1}$), different illumination regimes

(continuous illumination or alternation of light/dark periods of different durations), and culture methods (batch or continuous culture regimes) [32].

3.2.1. Studies on *Chlamydomonas reinhardtii*

Mus et al. [33] have been studied anaerobic acclimation in *C. reinhardtii*. In their study, metabolite, genomic, and transcriptome data were used in order to provide genome-wide insights into the regulation of the complex metabolic networks which utilized by *Chlamydomonas* under the anaerobic conditions associated with H₂ production.

Ghirardi and Seibert [34] have generated algal hydrogenase mutants with higher O₂ tolerance to function with aerobic H₂-production systems and they have optimized the rates of H₂ production.

Pai and Lai [6] made an analysis of algae growth and oil production in a batch reactor under high nitrogen and phosphorus conditions and discussed the feasibility for simultaneous local fresh water oleaginous algae cultivation and wastewater nitrogen removal.

Heifetz et al. [35] made a study about the effects of acetate on facultative autotrophy in *C. reinhardtii*. They illustrated that both photosynthetic incorporation of inorganic carbon and the maximum rate of O₂ evolution in *C. reinhardtii* can be significantly diminished by growth in the presence of acetate.

Fan et al. [36] investigated the regulatory factors controlling oil biosynthesis by the metabolic interconnection between starch and oil in *Chlamydomonas*. They have suggested that the carbon availability is a key metabolic factor controlling oil biosynthesis and carbon partitioning between starch and oil in *Chlamydomonas*.

Terashima et al. [37] studied the localisation currently known key proteins involved in the anaerobic response to within or outside of the chloroplast and identification of proteins significantly induced under anaerobiosis through quantitative proteomics.

Mitchell et al. [38] investigated ATP production in *C. reinhardtii* flagella by glycolytic enzymes. They have reported that *C. reinhardtii* flagella possess three enzymes of the lower half of the glycolytic pathway, allowing ATP production in situ from the glycolytic intermediate 3-phosphoglycerate. Additionally, they showed that enolase which is one of these enzymes is linked to the 9+2 microtubule scaffold (axoneme) through its association with the CPC1 central pair protein. Reductions in flagellar enolase in *cpc1* mutants correlate with reductions in motility due to reduced intraflagellar ATP concentrations. Also, they illustrated that the other two glycolytic enzymes, which are phosphoglycerate mutase and an unusual pyruvate kinase, are located in the membrane+matrix fraction.

Wemmer and Marshall [39] have studied the flagellar motility of *C. reinhardtii* by investigating the organisation of flagellum.

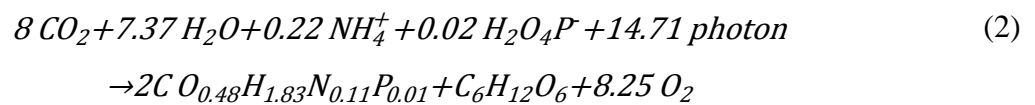
Tamburic et al. [40] studied the effect of the light regime and phototrophic conditions on growth of *C. reinhardtii*. They found that using 12h:12h light:dark cycles reduces the algal growth rate and cell density by approximately 30% compared to the values measured under continuous illumination since the algae cannot photosynthesise during the dark cycles and therefore tend to store their energy reserves rather than using them to grow and reproduce which means that large-scale outdoor photobioreactors will not be able to match the hydrogen production rates observed in laboratory reactors with access to continuous illumination.

Sorguven and Ozilgen [3] performed a thermodynamical analysis for the algae–biodiesel–carbon dioxide cycle. They investigated the biodiesel production with respect to their ability to produce useful work and to determine their impact on environment, hence it's sustainability.

4. METHODS

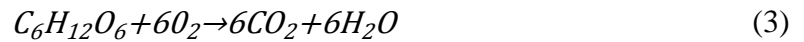
For the purposes of this study, the detailed chemistry is simplified as a three-step mechanism:

Photosynthesis:

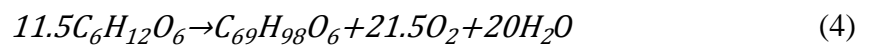


where 12.8-14.4% of solar energy may be considered to be converted into algal biomass [41].

Respiration:



Lipid production:



Reactions (3) and (4) are competitive where glucose is consumed either for respiration or for lipid production.

4.1. EXPERIMENTAL DATA

Equations (2) – (4) constitute the backbone of our analysis. The experimental data published by *Tevatia et al.*, 2012 [42] pertinent to growth and lipid production by *Chlamydomonas reinhardtii* at 18.7 mM, 6.2 mM, 0.7 mM, and 0 mM ammonium concentrations were employed in our analysis.

4.2. MODELING CONSIDERATIONS

Following assumptions were made in kinetic and thermodynamic modeling:

- The lipid production process in the tris-phosphate medium at 25°C is considered as an open system.
- Photosynthesis, respiration, and lipid production are regarded as the only reactions occurring within the system.
- Concentrations of glucose and carbon dioxide are assumed to remain constant in the system.
- The *Chlamydomonas reinhardtii* cell is considered to be spherical in shape, and the Reynolds numbers pertinent to its motion in the media is regarded to be small enough to permit calculation of the drag force on cell according to the Stoke's law.
- Temperature of the surroundings is assumed to be 25°C.

4.3. SYSTEM BOUNDARY

The system chosen in this study was a 1 L solution where *C.reinhardtii* was cultivated in TP medium. Concentrations of the chemicals were taken from the experimental work by *Tevatia et al.*, 2012 [42]. The temperature in the system boundary was 298 K. In the system boundary, reactions (2)-(4) occur.

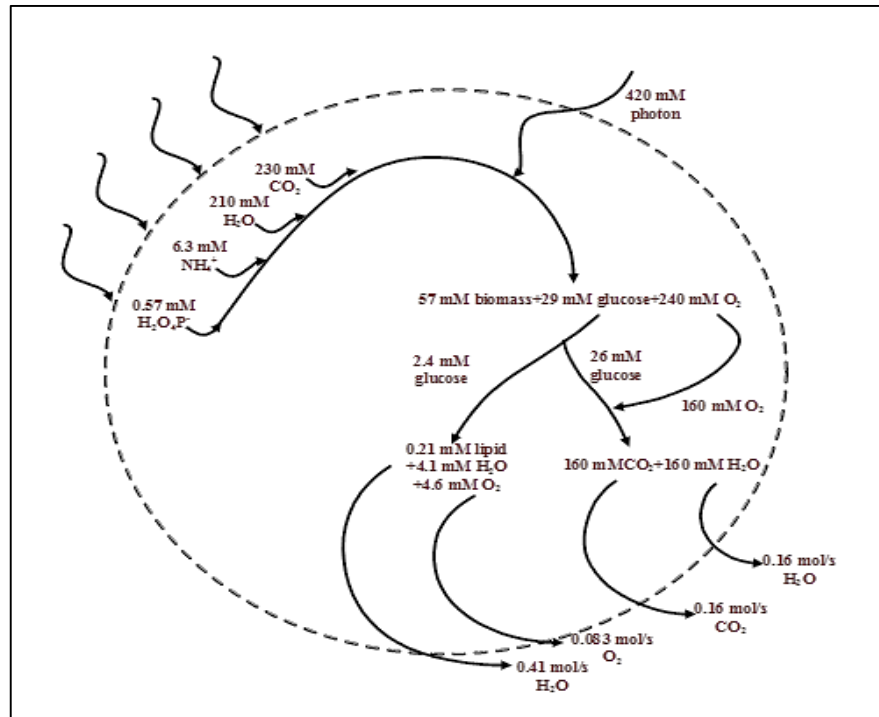


Figure 4.1. System boundary

4.4. KINETIC ANALYSIS

Kinetic models were employed as continuous mathematical functions relating lipid production to the microbial population. Only a fraction of the original data of *Tevatia et al.* (2012), which were considered most useful for our analysis, is adapted. The initial stages of cultivation when the amounts of biomass are low was not taken, therefore the time $t=0$ of the original data and those of our analysis were not the same; moreover the final stages of the original data, when the storage lipids are declining were not used. *Tevatia et al.*'s (2012) study presents rare sets of experimental data which permit both the calculation of the exergy input via photosynthesis and the flagella work, therefore adapted for our study. Within the adapted range of the data, the growth rate of *C. reinhardtii* was simulated with the logistic equation:

$$\frac{dx}{dt} = \mu x \left(1 - \frac{x}{x_{max}} \right) \quad (4.1)$$

The logistic growth model assumes that the growth of the systems propagates until an upper limit, x_{max} , is attained; meanwhile the growth rate decreases gradually, producing the

characteristic S-shape curve [43]. The rate of neutral lipid production was simulated with the Luedeking-Piret model:

$$\frac{dP}{dt} = \alpha x + \beta \frac{dx}{dt} \quad (4.2)$$

where the first term αx is related with the product formed in proportion with the size of the microbial population, and the next term, $\beta(dx/dt)$, implies that the additional product formation rate in proportion with the growth rate. The dimensionless constants α and β were obtained to minimize the sum of the square difference between the data and the model.

4.5. THERMODYNAMIC ANALYSIS

The following equations represent the 1st and 2nd law of thermodynamics for the control volume:

Mass balance:

$$\sum (\Delta N)_{in} - \sum (\Delta N)_{out} - \sum (\Delta N)_{acc} = 0 \quad (4.3)$$

Energy balance:

$$\frac{\Delta E_{sys}}{\Delta t} = \sum (\Delta Nh)_{in} - \sum (\Delta Nh)_{out} - \sum (\Delta Nh)_{acc} - \Delta Q = 0 \quad (4.4)$$

Exergy is not a conserved quantity. It is destroyed because of the internal and external irreversibilities.

Exergy balance:

$$\frac{\Delta X_{destroyed}}{\Delta t} = \sum (\Delta Nb)_{in} - \sum (\Delta Nb)_{out} - \sum (\Delta Nb)_{acc} + \Delta Q \left(1 - \frac{T_s}{T}\right) \quad (4.5)$$

The molecular weight, enthalpy of formation at 298 K, and standard chemical exergy data were tabulated at Table 1. The temperature which the reaction occurs is also 298 K, hence the enthalpy of formation data at 298 K was used and T_s is 298 K.

4.6. WORK

Chlamydomonas reinhardtii uses flagella for motility [44]. Flagellar work was calculated for one unit carbon formula of cell, and then multiplied with the estimates of the biomass from the kinetic analysis to determine the amount of the work done as a function of time. The motion of the individual cells is not affected by the presence of the others.

The drag force F_d was calculated according to the Stoke's law by assuming that the cell body is spherical since Reynolds number is very small [45, 46]:

$$F_d = -3\pi\eta dv \quad (4.6)$$

where η is the dynamic viscosity of the fluid (1.407×10^{-3} kg/m s) [47], d is the diameter of the cell (1×10^{-5} m) [48] and v is the average velocity of the cell (3×10^{-5} m/s) [49]. The drag force was multiplied by the average velocity and thus the work done by flagella was determined for one cell, and since the dry weight of algae cells is 5.5×10^6 cells/mg [50] and molecular weight of the cell is 23.36 g/mol (Table 1), the total flagella work was calculated for one mole of cell.

4.7. PHOTON ENERGY

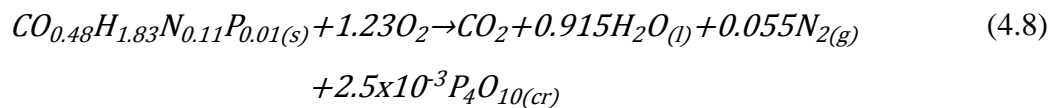
During cultivation 85 W Super High Output fluorescent lights was used to provide 200 $\mu\text{mol photons/m}^2\text{s}$ [42]. The energy of light was calculated by Equation (4.7) and the unit was converted to kJ/mol.

$$E = \frac{hc}{\lambda} \quad (4.7)$$

where h is the Planck's constant (6.626×10^{-34} J s), c is the speed of the light (2.9998×10^8 m/s) and λ is the wavelength of the radiation (555 nm). The bulb has a color temperature of 6500 K [51] which corresponds to daylight [52] hence exergy of sunlight was taken as 0.5155 kW/m^2 [53].

4.8. ESTIMATION OF THERMODYNAMIC PROPERTIES OF BIOCHEMICALS

The chemical formula of the bacterium is $\text{CO}_{0.48}\text{H}_{1.83}\text{N}_{0.11}\text{P}_{0.01}$ [54]; corresponding to 23.36 g/mol and *Battley's* (1999) [55] measurement of the heat of formation of the dry biomass from the combustion reaction for $\Delta H_{c,\text{cell}}$ for *Saccharomyces cerevisiae* as -19.44 kJ/g. The combustion reaction of the one unit carbon formula biomass and the enthalpy of the combustion for this reaction are:



$$\Delta H_{c,\text{cell}} = \Delta H_{f,\text{CO}_2(g)} + 0.915\Delta H_{f,\text{H}_2\text{O}_{(l)}} + 0.055\Delta H_{f,\text{N}_2(g)} + 2.5 \times 10^{-3}\Delta H_{f,\text{P}_4\text{O}_{10(cr)}} - \Delta H_{f,\text{cell}(s)} - 1.23\Delta H_{f,\text{O}_2(g)} \quad (4.9)$$

The heat of formation of the chemicals was tabulated on Table 1. The heat of formation of biomass was determined from Equation (4.9) as -201.79 kJ/mol.

Exergy of a substance is the maximum work that can be extracted from this substance if it is brought to thermal, mechanical and chemical equilibrium with its surroundings via

reversible processes. The exergy of a substance can be calculated as the sum of its chemical and physical exergy:

$$b = b_{ch} + h - h_0 + T_0(s - s_0) \quad (4.10)$$

The substances considered in the system are at the environmental temperature and pressure. Inlet and outlet streams are considered as ideal homogenous solutions. Therefore, enthalpy of a substance (h) is equal to its enthalpy at the dead state (h_0). There is a difference between the entropy of a substance and its entropy at the dead state, because the inlet and outlet streams have different compositions than the environment. Equation (4.11) can be rewritten as following for the considered system:

$$b = b_{ch} + RT_0 \ln(y) \quad (4.11)$$

Where R is the universal gas constant ($8.314 \text{ kJ kmol}^{-1} \text{ K}^{-1}$) and y is the fraction of the substance in the solution.

The chemical exergy of chemical species were taken from literature [56], except for the lipid, which is calculated based on a correlation suggested by *Moran et al.* [57]. Chemical exergy content of a substance can be calculated based on the known chemical exergy values of the products at the true dead state. For liquid hydrocarbon fuels of the type C_zH_y , chemical exergy can be predicted with the following equation [57]:

$$e^{ch} = LHV \left(1.042224 + 0.011925 \frac{y}{z} - \frac{0.042}{z} \right) \quad (4.12)$$

where LHV abbreviates the lower heating value.

Eco-exergy of the biomass was calculated the same way as [58]:

$$Eco\text{-exergy} = \sum_{i=1}^{i=n} \beta_i c_i \quad (4.13)$$

where the exergy factor $\beta=20$ for algae, as dictated by its genetic information, and c_i is the concentration of the biomass.

4.9. OPTICAL EXERGY LOSS

Lambert Beer law [59] relates the scatter of the incoming light to the particle concentration in a suspension. If we can consider that this relation is relevant to the increase of the algal concentration in the medium, we may estimate the exergy loss with the increase of the algal population as [60]:

$$A = \log\left(\frac{I}{I_0}\right) = \epsilon cl \quad (4.14)$$

where ϵ is the extinction coefficient ($37.93 \text{ M}^{-1}\cdot\text{cm}^{-1}$) [61], c is the concentration of biomass (mol/L) and l is the diameter of the reactor (17.9 cm). The exergy of the fraction of photon reflected, transmitted or scattered was calculated as [62]:

$$E_{optical\ loss} = b_{photon} \times \left(1 - \frac{A_0}{A}\right) \quad (4.15)$$

4.10. CUMULATIVE DEGREE OF PERFECTION (CDP)

The cumulative degree of perfection (CDP) is the ratio of the chemical exergy of the product to the sum of the exergies of all the raw materials and the fuel consumed during production [56]:

$$CDP_{lipid} = \frac{nb_{lipid}^o}{\sum nb_{reactants}^o} \times 100 \quad (21)$$

$$CDP_{biomass} = \frac{nb_{biomass}^o}{\sum nb_{reactants}^o} \times 100 \quad (22)$$

5. RESULTS

5.1. KINETIC MODEL

The algal growth was modeled with the logistic model and the lipid production is modeled with the Luedeking-Piret model. The models were compared with the experimental data in Figure 5.1. It is of crucial importance at this stage to relate the algal growth to lipid production with as little error as possible, since the error will propagate to the thermodynamic analysis. The constants of the kinetic model were tabulated in Table B.1. In the process where $[\text{NH}_4^+] = 18.7$ mM, the maximum biomass concentration, x_{max} attained is 8.08 g/L and with the lipid production of 1.34×10^{-2} g/L, in the process where $[\text{NH}_4^+] = 6.2$ mM, the maximum biomass concentration, x_{max} is 6.45 g/L with maximum lipid production of 3.7×10^{-3} g/L, in the case where $[\text{NH}_4^+] = 0.7$ mM, the maximum biomass concentration, x_{max} attained is 2.27 g/L and the achievement of 2.51×10^{-1} g/L lipid production and in the case where $[\text{NH}_4^+] = 0$ mM, the maximum biomass concentration, x_{max} attained is 1.34 g/L with the maximum lipid production of 2.10×10^{-1} g/L. The standard errors tabulated in Table B.2 were regarded to be small enough to go to the next stage of the analysis.

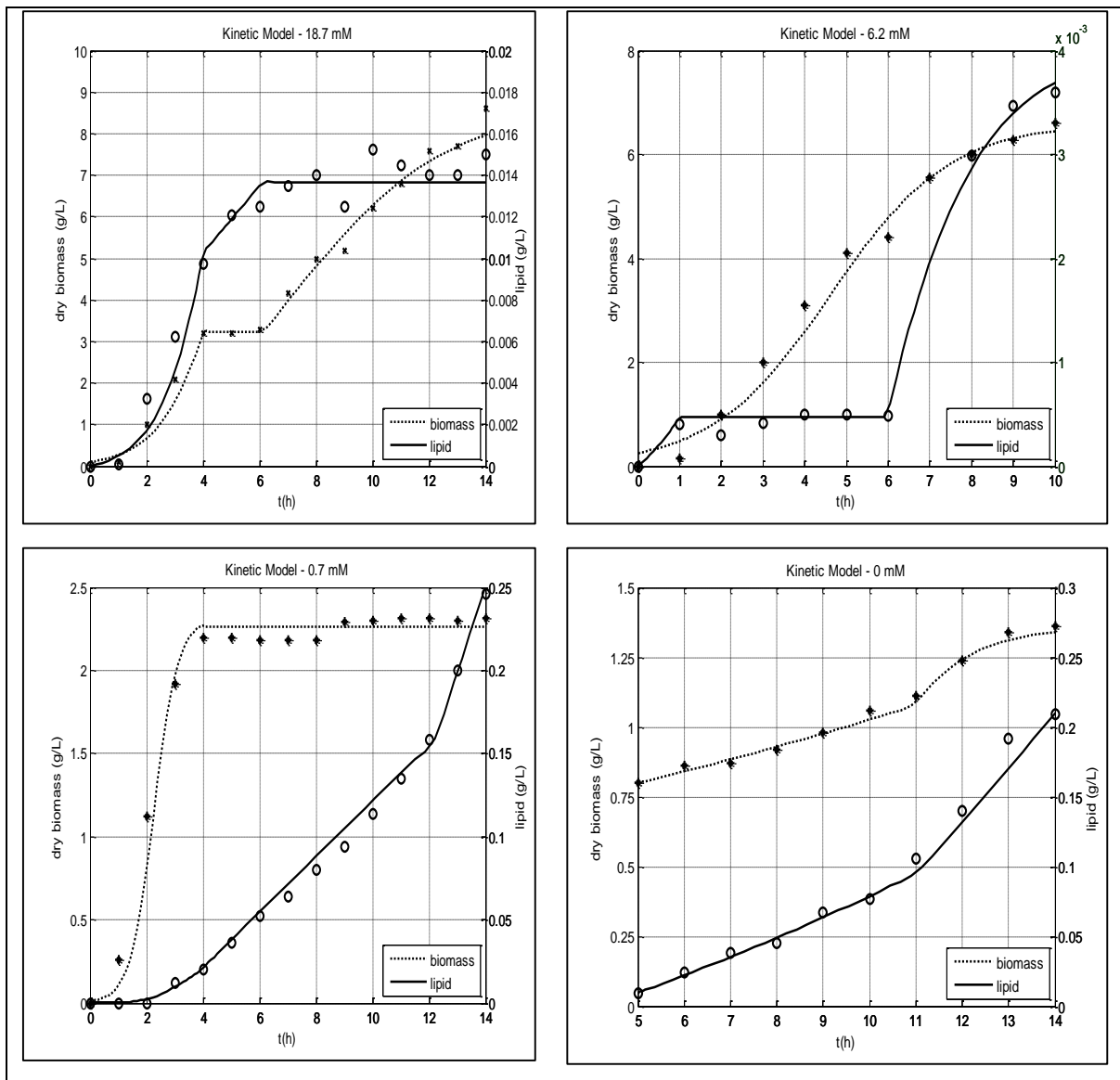


Figure 5.1. Simulation of kinetic model of *Chlamydomonas reinhardtii*

5.2. WORK

The algae do flagella work to move around, which was determined by drag force acting on the organism as -3.98×10^{-12} Pa by using Stoke's law. The alga was assumed to be spherical, and the Reynolds number is very small [45, 46], then the total work of one mole of cell was calculated as 1.3×10^{-3} kJ/mol. Flagellar work was determined as 5.29×10^{-5} kJ/g biomass, 5.59×10^{-5} kJ/g biomass, 5.61×10^{-5} kJ/g biomass, 5.54×10^{-5} kJ/g biomass for the cases when $[\text{NH}_4^+] = 18.7$ mM, $[\text{NH}_4^+] = 6.2$ mM, $[\text{NH}_4^+] = 0.7$ mM, and $[\text{NH}_4^+] = 0$ mM, respectively. These results imply that the maximum work is done when $[\text{NH}_4^+] = 0.7$ mM.

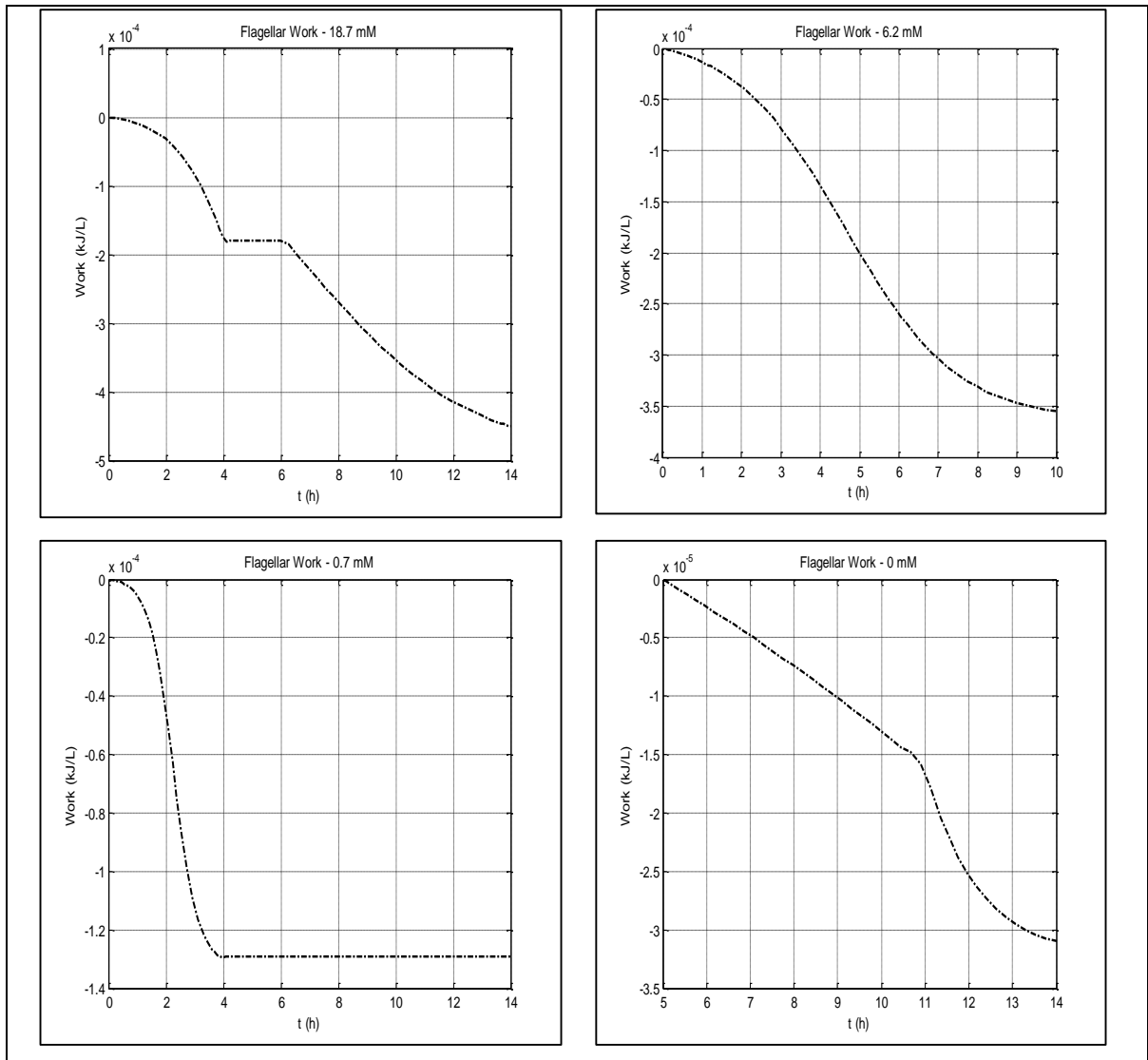


Figure 5.2. Simulation of flagellar work of *Chlamydomonas reinhardtii*

5.3. ENERGY LOSS

Reactions occur at 298 K by absorbing the light. There is a metabolic heat loss from the system. As listed in Table B.3, when $[\text{NH}_4^+]=18.7$ mM, heat loss from the system is 30.33 kJ/g biomass, when $[\text{NH}_4^+]=6.2$ mM, heat loss from the system is 32.09 kJ/g biomass, and when $[\text{NH}_4^+]=0.7$ mM, heat loss from the system is 27.76 kJ/g biomass, and when $[\text{NH}_4^+]=0$ mM, heat loss from the system is 17.00 kJ/g biomass.

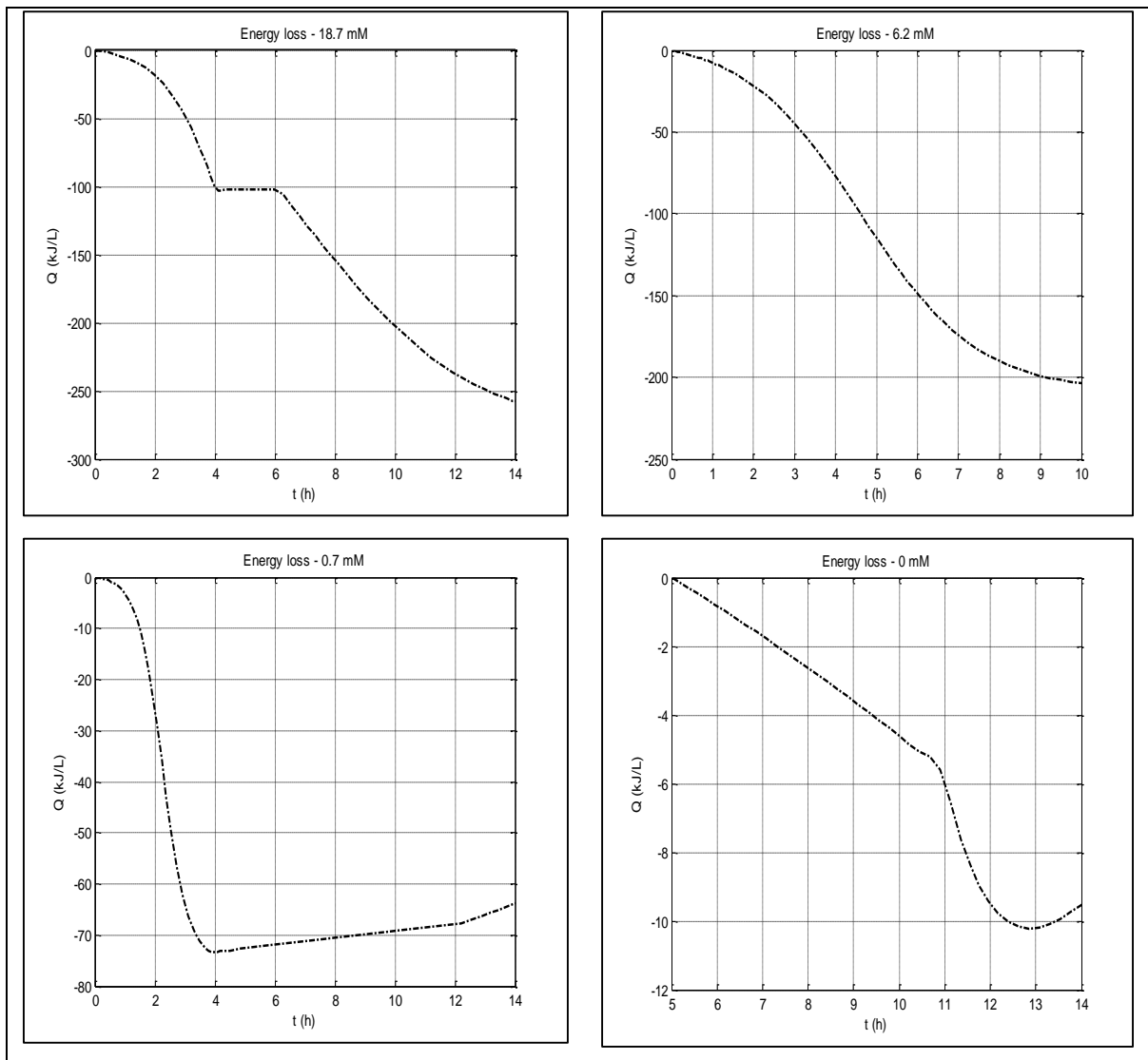


Figure 5.3. Simulation of energy loss of *Chlamydomonas reinhardtii*

5.4. EXERGY DESTRUCTION

It is almost customary to refer to the exergy destruction within a system due to internal irreversibilities [3, 4, 16, 17, 63, 64]. The group contribution method is based on the chemical structure, which can only be expressed by means of the unit carbon formula, but the exact structure is still cannot be detailed in high accuracy. The flagellar work helps the algae to locate themselves to capture more light, to improve in expense of the exergy of performing the work. Equation (4.5) represents the relation between heat and exergy destruction. As it can be seen in Table B.3, the amount of exergy destroyed is 739.46 kJ/g biomass for the case where $[\text{NH}_4^+] = 18.7 \text{ mM}$, 806.65 kJ/g biomass for the case where

$[\text{NH}_4^+]=6.2$ mM, 793.09 kJ/g biomass for the case where $[\text{NH}_4^+]=0.7$ mM and 636.82 kJ/g biomass for the case where $[\text{NH}_4^+]=0$ mM. Exergy of a system is referred as the maximum work which the system can produce when it is brought to thermal, mechanical and chemical equilibrium with its surroundings via reversible processes (Figure 5.5) [3] and it is proportional to the heat loss meaning that the heat loss causes exergy destruction and thus the available work lost.

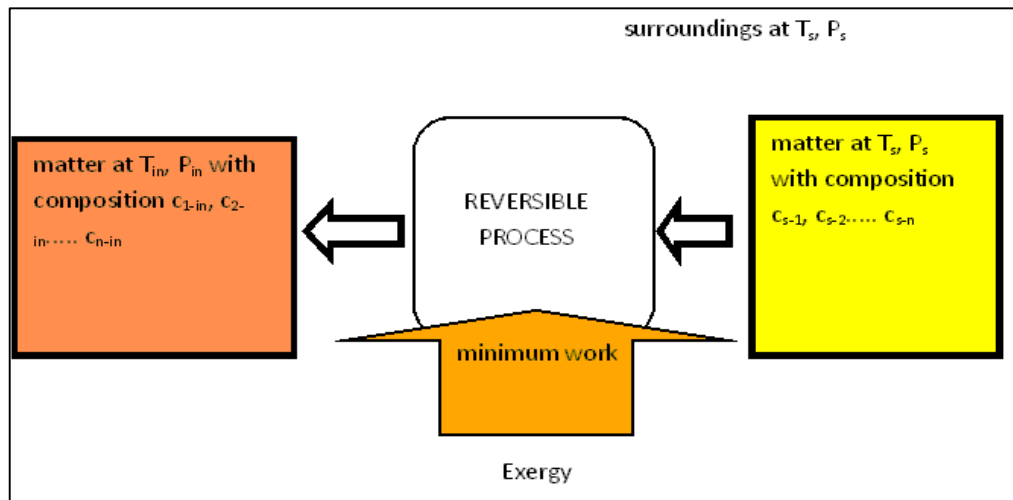


Figure 5.4. Concept of exergy in relation with our use in the given system

Hence, the case in which heat loss and exergy destruction are maximum is the case where $[\text{NH}_4^+]=6.2$ mM and $[\text{NH}_4^+]=0$ mM, respectively.

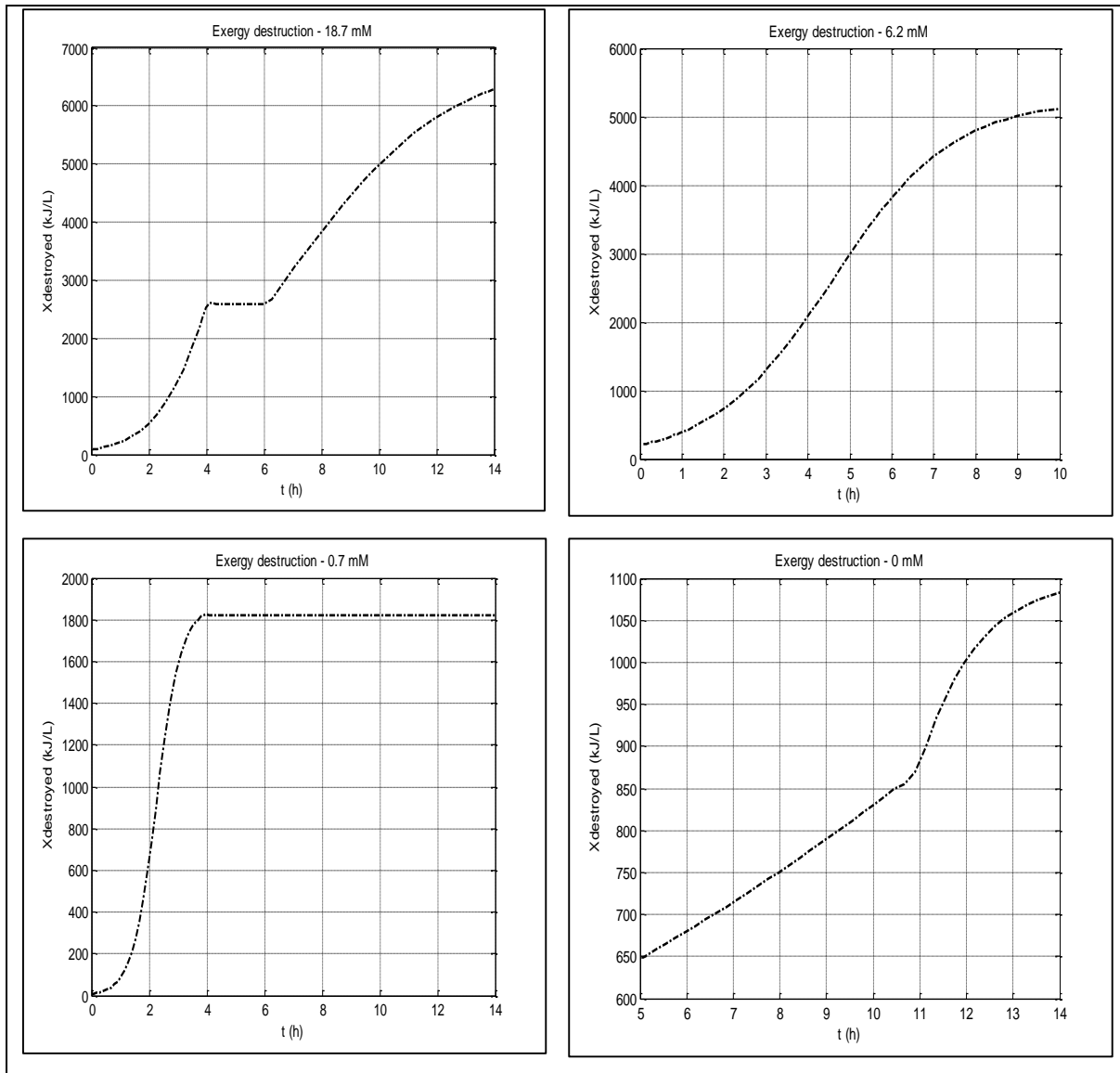


Figure 5.5. Simulation of exergy destruction of *Chlamydomonas reinhardtii*

5.5. ECO-EXERGY

Eco-exergy which is considered as the work capacity possessed by the organisms and the contribution to the eco-exergy of the ecosystem by the organisms was calculated as 8.01×10^{-1} kJ/g biomass, 8.69×10^{-1} kJ/g biomass, 8.43×10^{-1} kJ/g biomass, and 2.05 kJ/g biomass for the cases where $[\text{NH}_4^+] = 18.7$ mM, $[\text{NH}_4^+] = 6.2$ mM, $[\text{NH}_4^+] = 0.7$ mM and $[\text{NH}_4^+] = 0$ mM, respectively by equation (4.14) meaning that the maximum eco-exergy was determined in the case where $[\text{NH}_4^+] = 0.7$ mM. Additionally, work and eco-exergy were found to be parallel as it can be seen in Table B.3.

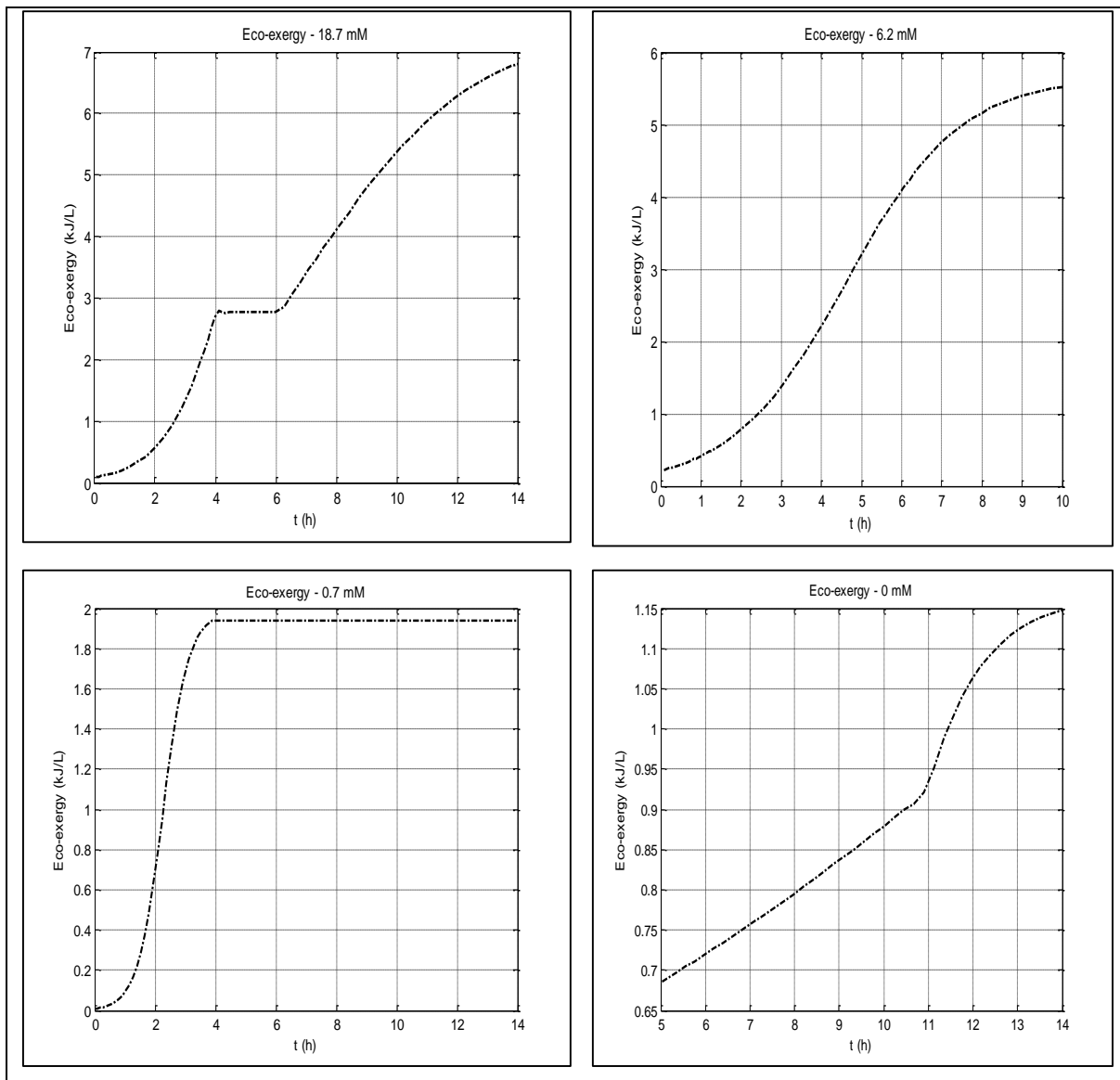


Figure 5.6. Simulation of eco-exergy of *Chlamydomonas reinhardtii*

5.6. OPTICAL EXERGY LOSS

The exergy of the fraction of photon reflected or transmitted was calculated by Lambert-Beer law which relates the scatter of the incoming light to the particle concentration in a suspension as 101.78 kJ/g biomass, 107.50 kJ/g biomass, 108.23 kJ/g biomass, and 106.11 kJ/g biomass for the cases where $[\text{NH}_4^+]=18.7$ mM, $[\text{NH}_4^+]=6.2$ mM, $[\text{NH}_4^+]=0.7$ mM and $[\text{NH}_4^+]=0$ mM, respectively.

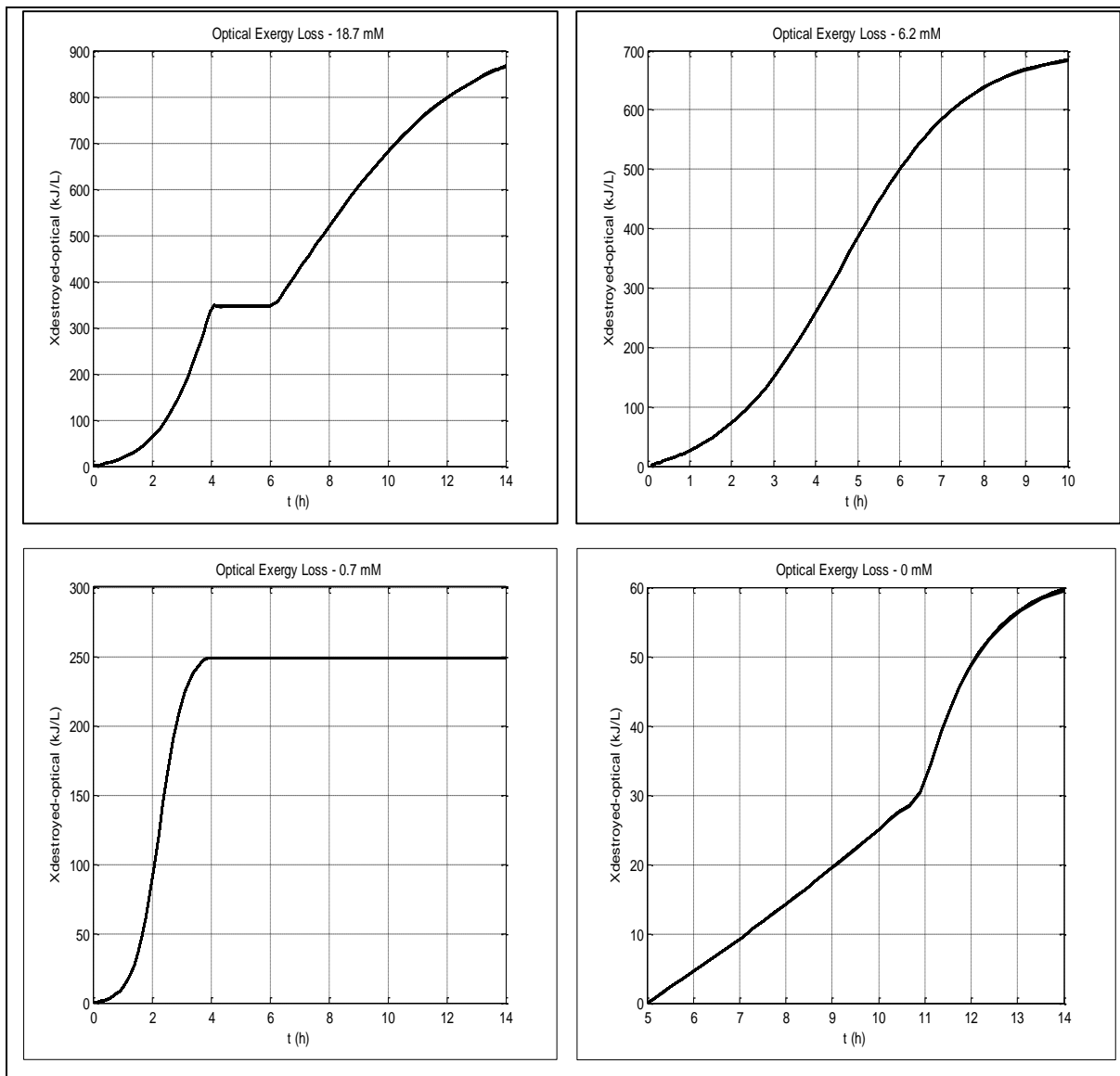


Figure 5.7. Simulation of optical exergy loss of *Chlamydomonas reinhardtii*

5.7. CUMULATIVE DEGREE OF PERFECTION (CDP)

CDP represents the measure of the deviation from thermodynamic ideals of a series of production processes from recovery of raw materials through the achievement of the desired products. A process sticking to the thermodynamic ideals has a higher CDP. Many processes have low efficiency results since every system comprises irreversibilities [65]. Therefore, renewable resources have higher CDP than non-renewable resources since they require a large amount of work to be spent in eco-systems [66]. CDP was calculated and scattered for both biomass and neutral lipid production (Figure 5.8). As it can be seen in

the figure, CDP for lipid production is much higher than that of biomass production. The case having highest CDP for lipid production is the case where $[\text{NH}_4^+]=0$ mM and the case where $[\text{NH}_4^+]=6.2$ mM has the highest CDP for biomass production (Table B.3). CDP of lipid production is 10.24% for the case where $[\text{NH}_4^+]=18.7$ mM, 16.05% for the case where $[\text{NH}_4^+]=6.2$ mM, 15.61% for the case where $[\text{NH}_4^+]=0.7$ mM and 25.55% for the case where $[\text{NH}_4^+]=0$ mM which indicates that the most efficient process due to lipid production is the case where $[\text{NH}_4^+]=0$ mM and the least efficient process is the case where $[\text{NH}_4^+]=18.7$ mM. In spite the high exergy destruction, the case where $[\text{NH}_4^+]=0$ mM is the most efficient process for lipid production (Table B.3). CDP of biomass production is 5.50×10^{-1} % for the case where $[\text{NH}_4^+]=18.7$ mM, 7.10×10^{-1} % for the case where $[\text{NH}_4^+]=6.2$ mM, 3.40×10^{-1} % for the case where $[\text{NH}_4^+]=0.7$ mM and 4.10×10^{-1} % for the case where $[\text{NH}_4^+]=0$ mM indicating that the most efficient process due to lipid production is the case where $[\text{NH}_4^+]=0$ mM and the least efficient process is the case where $[\text{NH}_4^+]=18.2$ mM.

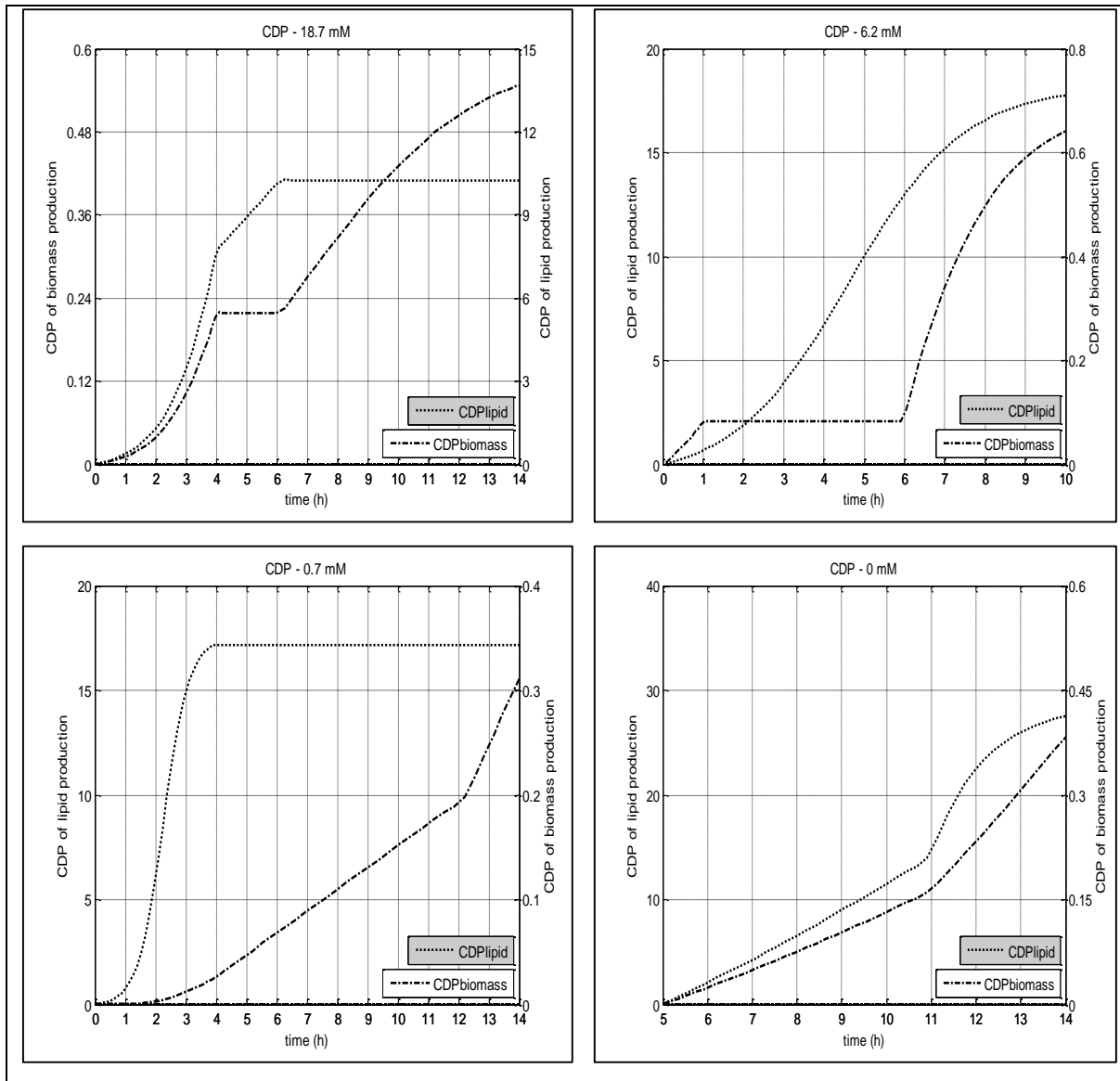


Figure 5.8. Simulation of CDP of *Chlamydomonas reinhardtii*

6. CONCLUSION

In this study, the biological activities of *C.reinhardtii* were examined via thermodynamical analysis to investigate the efficiency of lipid production by *C.reinhardtii* cultivation under four different conditions where $[\text{NH}_4^+]=18.7$ mM, $[\text{NH}_4^+]=6.2$ mM, $[\text{NH}_4^+]=0.7$ mM, and $[\text{NH}_4^+]=0$ mM. The results for 1 L of solution and 1 g of biomass differ due to the biomass efficiency. In the case where $[\text{NH}_4^+]=6.2$ mM, maximum work was observed. Results of thermodynamic analysis shows that the largest heat loss and exergy destruction per unit biomass production was designated in the case where $[\text{NH}_4^+]=6.2$ mM and this means thermodynamically inadequate conditions including release of high amounts of energy and destruction of exergy. The case where $[\text{NH}_4^+]=0$ mM having the highest exergetic efficiency of neutral lipid production has the least heat loss and relatively low exergy destruction. Eco-exergy of biomass is very low while the exergy destruction is high since it means the available work loss within the system, and this supports the inverse relationship between eco-exergy and exergy destruction. Additionally, the case where $[\text{NH}_4^+]=0.7$ mM has the highest optical exergy loss while minimum CDP of biomass production since a fraction of solar energy is considered to be converted into algal biomass. The case having the maximum CDP of lipid production and CDP has lower of biomass production, therefore it can be concluded that neutral lipid production takes place under nitrogen depleted conditions. Hence, for further processes to produce biofuel cultivation under the condition where $[\text{NH}_4^+]=0$ mM would be chosen.

REFERENCES

1. Stryer, L., *Biochemistry*, 2nd ed., W.H. Freeman, San Francisco, 1981.
2. Lehninger, A. L., *Principles of Biochemistry*, Worth Pub, New York, 1982.
3. Sorgüven, E., Özilgen, M., “Thermodynamic assessment of algal biodiesel utilization”, *Renewable Energy*, Vol. 35, pp. 1956-1966, 2010.
4. Sorgüven, E., Özilgen, M., Thermodynamic efficiency of synthesis, storage and breakdown of the high-energy metabolites by photosynthetic microalgae”, *Energy*, Vol. 58, pp. 679-687, 2013.
5. Maul, J.E., Lilly, J.W., Cui, L., dePamphilis, C.W., Miller, W., Harris, E.H., Stern, D.B., “The *Chlamydomonas reinhardtii* plastid chromosome: Islands of genes in a sea of repeats”, *The Plant Cell*, Vol. 14, pp. 2659-2679, 2002.
6. Pai, T.Y., Lai, W.J., “Analyzing Algae Growth and Oil Production in a Batch Reactor under high Nitrogen and Phosphorus Conditions”, *International Journal of Applied Science and Engineering*, Vol. 9 (3), pp. 161-168, 2011.
7. Ayres, R.U., “Eco-thermodynamics: Economics and The Second Law”, *Ecological Economics*, Vol. 26, pp. 189-209, 1998.
8. Ayres, R.U., “The second law, the fourth law, recycling and limits to growth”, *Ecological Economics*, Vol. 29 (3), pp. 473-483, 1999.
9. Caton, J.A, A review of investigations using the second law of thermodynamics to study internal combustion engines, *SAE technical paper No. 2000-01-1081*, Warrendale, PA: Society of Automotive Engineers Inc., 2000.

10. Rakopoulos, C.D., Giakoumis, E.G., “Second-law analyses applied to internal combustion engines operation”, *Progress in Energy and Combustion Science*, Vol. 32, 32, pp. 2-47, 2006.
11. Talens, L., Villalba, G., Gabarrell, X., “Exergy analysis applied to biodiesel production”, *Resources Conservation and Recycling*, Vol. 51, pp. 397-407, 2007.
12. Jubrias, S.A., Vollestad, N.K., Gronka, R.K., Kushmerick, M.J., “Contraction coupling efficiency of human first dorsal interosseous muscle”, *The Journal of Physiology*, Vol. 586 (7), pp. 1993-2002, 2008.
13. Lems, S., van der Kooi, H.J., de Swaan Arons, J., “The second-law implications of biochemical energy conversion: exergy analysis of glucose and fatty-acid breakdown in the living cell”, *International Journal of Exergy*, Vol. 6 (2), pp. 228-248, 2009.
14. Mady, C.E.K. and Oliveira, Jr., S. “Human body exergy metabolism”, *Proceedings of ECOS 2012 – The 25th International conference on efficiency, cost, optimization, simulation and environmental impact of energy systems*, Perugia, Italy, 2012, Vol. 160, pp. 1-13.
15. Mady, C.E.K., Ferreira, M.S., Yanagihara, J.I., Saldiva P.H.N., Oliveira, Jr., S., “Modeling the exergy behavior of human body”, *Energy*, Vol. 45, pp. 546-553, 2012.
16. Genc, S., Sorgüven, E., Kurnaz, Aksan, I., Özilgen, M., “Exergetic efficiency of ATP production in neuronal glucose metabolism”, *International Journal of Exergy*, Vol. 13 (1), pp. 60-84, 2013.
17. Genc, S., Sorgüven, E., Özilgen, M., Kurnaz, Aksan, I., “Unsteady exergy destruction of the neuron under dynamic stress conditions”, *Energy*, Vol. 59, pp. 422-431, 2013.
18. von Stockar, U. and van der Wielen, L. A.M., “Thermodynamics in biochemical engineering”, *Journal of Biotechnology*, Vol. 59, pp. 25-37, 1997.

19. von Stockar, U., Liu, J.S., “Does microbial life always feed on negative entropy? Thermodynamic analysis of microbial growth”, *BBA-Bioenergetics*, Vol. 1412 (3), pp. 191-211, 1999.
20. Battley, E. H., “The development of direct and indirect methods for the study of the thermodynamics of microbial growth”, *Thermochimica Acta*, Vol. 309, pp. 17-37, 1998.
21. Trevors, J.T., “Origin of microbial life: Nano- and molecular events. thermodynamics/entropy. Quantum mechanisms and genetic instructions”, *Journal of Microbiological Methods*, Vol. 82, pp. 492-495, 2011.
22. von Stockar, U., Vojinovic, V, Maskow, T. and Liu, J., “Can microbial growth yield be estimated using simple thermodynamic analogies to technical processes?”, *Chemical Engineering and Processing*, Vol. 47, pp. 480-490, 2008.
23. von Stockar, U., Maskow, T., Liu, J., Marison, I. W. and Patino, R., “Thermodynamics of microbial growth and metabolism: An analysis of the current situation”, *Journal of Biotechnology*, Vol. 121, pp. 517-533, 2006.
24. “Biofuels: What are they?,” Biofuels [online], 2010, <http://www.biofuel.org.uk/> [retrieved 27 January 2014].
25. “Biofuels A Solution for Climate Change,” U.S. Department of Energy [online], 1999, <http://www.nrel.gov/docs/fy99osti/24052.pdf> [retrieved 27 January 2014].
26. “Biodiesel from Algae Oil,” MicrobeWiki [online], 2011, http://microbewiki.kenyon.edu/index.php/Biodiesel_from_Algae_Oil. [retrieved 27 January 2014].
27. Ryan, C., “Cultivating Clean Energy: The Promise of Algae Biofuels,” Natural Resources Defense Council [online], 2009, <http://www.nrdc.org/energy/files/cultivating.pdf> [retrieved 27 January 2014].

28. Hu, Q., Sommerfeld, M., Jarvis, E., Ghirardi, M., Posewitz, M., Seibert, M., Darzins, A., “Microalgal triacylglycerols as feedstocks for biofuel production: perspectives and advances”, *The Plant Journal*, Vol. 54, pp. 621–639, 2008.
29. “*Chlamydomonas reinhardtii*,” Davidson College [online], <http://www.bio.davidson.edu/courses/molbio/molstudents/coble/cobleintro.html>. [retrieved 27 January 2014].
30. Hemschemeier, A.C., “The anaerobic life of the photosynthetic alga *Chlamydomonas reinhardtii* Photofermentation and hydrogen production upon sulphur deprivation,” Massachusetts Institute of Technology [online], 2005, http://web.mit.edu/pweigele/www/PBR_background/dissertation_anaerobic_chlamy.pdf. [retrieved 27 January 2014].
31. Silflow, C.D., Lefebvre, P.A., “Assembly and Motility of Eukaryotic Cilia and Flagella. Lessons from *Chlamydomonas reinhardtii*”, *Plant Physiology*, Vol. 127, pp. 1500-1507, 2001.
32. Vitova, M., Bisova, K., Hlavova, M., Kawano, S., Zachleder, V., Cizkova, M., “*Chlamydomonas reinhardtii*: duration of its cell cycle and phases at growth rates affected by temperature”, *Planta*, Vol. 234, pp. 599–608, 2011.
33. Mus, F., Dubini, A., Seibert, M., Posewitz, M.C., Grossman, A.R., “Anaerobic Acclimation in *Chlamydomonas Reinhardtii* Anoxic Gene Expression, Hydrogenase Induction, And Metabolic Pathways”, *The Journal of Biological Chemistry*, Vol. 282 (35), pp. 25475–25486, 2007.
34. Ghirardi, M.L., Seibert, M., “Algal Systems for Hydrogen Photoproduction,” Office of Energy Efficiency&Renewable Energy [online], 2003, http://www1.eere.energy.gov/hydrogenandfuelcells/pdfs/iic3_ghirardi.pdf [retrieved 27 January 2014].

35. Heifetz, P.B., Förster, B., Osmond, C.B., Giles, L.J., Boynton, J.E., “Effects of acetate on facultative autotrophy in *Chlamydomonas reinhardtii* assessed by photosynthetic measurements and stable isotope analyses”, *Plant Physiology*, Vol. 122 (4), pp. 1439-1445, 2000.
36. Fan, J., Yan, C., Andre, C., Shanklin, J., Schwender, J., Xu, C., “Oil accumulation is controlled by carbon precursor supply for fatty acid synthesis in *Chlamydomonas reinhardtii*”, *Plant Cell Physiology*, Vol. 53 (8), pp. 1380–1390, 2012.
37. Terashima, M., Specht, M., Naumann, B., Hippler, M., “Characterizing the Anaerobic Response of *Chlamydomonas reinhardtii* by Quantitative Proteomics”, *Molecular & Cellular Proteomics*, Vol. 9 (7), pp. 1514-1532, pp. 2010.
38. Mitchell, B.F., Pedersen, L.B., Feely, M., Rosenbaum, J.L., Mitchell, D.R., “ATP Production in *Chlamydomonas reinhardtii* Flagella by Glycolytic Enzymes”, *Molecular Biology of the Cell*, Vol. 16, pp. 4509–4518, 2005.
39. Wemmer, K.A., Marshall, W.F., “Flagellar Motility: All Pull Together”, *Current Biology*, Vol. 14, 2004.
40. Tamburic, B., Zemichael, F.W., Maitland, G.C., Hellgardt, K., “Effect of the light regime and phototrophic conditions on growth of the H₂-producing green alga *Chlamydomonas reinhardtii*”, *Energy Procedia*, Vol. 29, pp. 710-179, 2012.
41. Asmare, A.M., Demessie, B.A., Murthy, G.S., “Theoretical Estimation the Potential of Algal Biomass for Biofuel Production and Carbon Sequestration in Ethiopia”, *International Journal of Renewable Energy Research*, Vol. 3 (3), 2013.
42. Tevatia, R., Demirel, Y., Blum, P., “Kinetic modeling of photoautotrophic growth and neutral lipid accumulation in terms of ammonium concentration in *Chlamydomonas reinhardtii*”, *Bioresource Technology*, Vol. 119, pp.419–424, 2012.

43. Bailey, J.E., Ollis, D.F., *Biochemical Engineering Fundamentals*, 2nd ed, McGraw-Hill, USA, 1986.
44. Silflow, C.D., Lefebvre, P.A., “Assembly and motility of eukaryotic cilia and flagella. Lessons from *Chlamydomonas reinhardtii*”, *Plant Physiology*, Vol. 127, pp. 1500-1507, 2001.
45. Loth E., “Drag of non-spherical solid particles of regular and irregular shape”, *Powder Technology*, Vol. 182, pp. 342-353, 2008.
46. Martinez, V.A., Besseling, R., Croze, O.A., Tailleur, J., Reufer, M., Schwarz-Linek, J., Wilson, L.G., Bees, M.A., Poon, W.C.K., “Differential Dynamic Microscopy: A High-Throughput Method for Characterizing the Motility of Microorganisms”, *Biophysical Journal*, Vol. 103, pp. 1637-1647, 2012.
47. Córdoba-Castro, N.M., Montenegro-Jaramillo, A.M., Prieto, R.E., González-Mariño, G.E., “Analysis Of The Effect Of The Interactions Among Three Processing Variables For The Production Of Exopolysaccharides In The Microalgae *Scenedesmus obliquus* (UTEX 393)”, *Vitae*, Vol. 19 (1), 2012.
48. Kurtuldu, H., Guasto, J.S., Johnson, K.A., Gollub, J.P., “Enhancement of biomixing by swimming algal cells in two-dimensional films”, *Proceedings of the National Academy of Sciences*, Vol. 108 (26), pp. 10391–10395, 2011.
49. Kantsler, V., Dunkel, J., Polin, M., Goldstein, R.E., “Ciliary contact interactions dominate surface scattering of swimming eukaryotes”, *Proceedings of the National Academy of Sciences of the United States of America*, 2012.
50. Jensen, T.E., Sicko-Goad, L., “Aspects of phosphate utilization by blue-green algae”, *Ecological Research Series*, 1976.
51. “Lights of America. 85W FLOUREX Replacement Bulb,” Lights of America [online], <http://www.lightsofamerica.com/Products/9385B.aspx>; 2014 [retrieved 11 April 2014].

52. “What is the light colour temperature($^{\circ}$ K)?,” The Daylight Company [online], 2009, <https://uk.daylightcompany.com/information/Kelvin/> [retrieved 11 April 2014].
53. Petela, R., “An approach to the exergy analysis of photosynthesis”, *Solar Energy*, Vol. 82, pp. 311-328, 2008.
54. Baliga, R., Powers, S.E., “Sustainable Algae Biodiesel Production in Cold Climates”, *International Journal of Chemical Engineering*, 2010.
55. Battley, E.H., “An empirical method for estimating the entropy of formation and the absolute entropy of dried microbial biomass for use in studies on the thermodynamics of microbial growth”, *Thermochimica Acta*, Vol. 326, pp. 7–15, 1999.
56. Szargut, J., Morris, D.R., Steward, F.R., *Exergy Analysis of Thermal, Chemical, and Metallurgical Processes*, Hemisphere, New York, 1988.
57. Moran, M.J., *Availability Analysis: A Guide to Efficient Energy Use*. Prentice-Hall, Englewood Cliffs, NJ, 1982.
58. Jorgensen, S.E., Ludovisi, A., Nielsen, S.N., “The free energy and information embodied in the amino acid chains of organisms”, *Ecological Modelling*, Vol. 221, pp. 2388-2392, 2010.
59. Rybynok, V.O., Kyriacou, P.A., “Beer-Lambert law along non-linear mean light pathways for the rational analysis of Photoplethysmography”, *Journal of Physics: Conference series*, Vol. 238, 2010.
60. Clark, J. “The Beer-Lambert Law” [online], <http://www.chemguide.co.uk/analysis/uvvisible/beerlambert.html>; 2007 [retrieved 21 May 2014].

61. Hannis, K., *Optical behavior of algae particles in photobioreactors*, M.S. Report, Delft University of Technology, 2013.
62. Sassaroli, A., Fantini, S., “Comment on the modified Beer-Lambert law for scattering media”, *Physics in Medicine and Biology*, Vol. 49, pp. 255-257, 2004.
63. Sorgüven, E., Özilgen, M., “Energy utilization, carbon dioxide emission, and exergy loss in flavored yogurt production process”, *Energy*, Vol. 40, pp. 214-225, 2012.
64. Degerli, B., Küçük, K., Sorgüven, E., Özilgen, M., “Thermodynamic analysis of serogroup C antigen production by *Neisseria Meningitidis*”, *International Journal of Exergy*, 2014; accepted for publication, in press.
65. Kleidon, A., Lorenz, R., Lorenz, R.D., *Non-equilibrium Thermodynamics and the Production of Entropy: Life, Earth and Beyond*, Springer, Germany, 2005.
66. Suh, S., *Handbook of Input-Output Economics in Industrial Ecology*, Vol. 23, Springer, 2009.
67. “ α -D-Glucose,” National Institute of Standards and Technology Chemistry Webbook [online database], <http://webbook.nist.gov/cgi/cbook.cgi?ID=C492626&Mask=2> [retrieved 21 January 2014].
68. “Oxygen,” National Institute of Standards and Technology Chemistry Webbook [online database], <http://webbook.nist.gov/cgi/cbook.cgi?ID=C7782447> [retrieved 21 January 2014].
69. “H₂PO₄ anion,” National Institute of Standards and Technology Chemistry Webbook [online database], <http://webbook.nist.gov/cgi/cbook.cgi?ID=B4100&Units=CAL&Mask=20> [retrieved 21 January 2014].

70. “NH₄+,” National Institute of Standards and Technology Chemistry Webbook [online database],

<http://webbook.nist.gov/cgi/cbook.cgi?ID=C14798039&Mask=800> [retrieved 21 January 2014].

71. “Water,” National Institute of Standards and Technology Chemistry Webbook [online database],

<http://webbook.nist.gov/cgi/cbook.cgi?ID=C7732185> [retrieved 21 January 2014].

72. “Carbon dioxide,” National Institute of Standards and Technology Chemistry Webbook [online database],

<http://webbook.nist.gov/cgi/cbook.cgi?ID=124389> [retrieved 21 January 2014].

73. Chang, R., Piepho, S., Chapter 6, Worksheet 2, *Chemistry*, 8th ed., McGraw-Hill College, 2004.

74. “Reactions: Heat of Formation Table,” Web Portal for Thermodynamic Properties [online database],

<http://thermo.sdsu.edu/testhome/Test/solve/basics/tables/tablesComb/formation.html> [retrieved 21 January 2014].

75. “Heats of Formation Table,” Chemistry About [online],

<http://chemistry.about.com/od/chartstables/a/heatofformions.htm> [retrieved 21 January 2014].

76. “Standard Enthalpy of Formation,” UC Davis ChemWiki [online],

http://chemwiki.ucdavis.edu/Physical_Chemistry/Thermodynamics/State_Functions/Enthalpy/Standard_Enthalpy_Of_Formation [retrieved 21 January 2014].

77. Stokes, R.D., *Exergy Modeling to Compare Engineered Products to Biological Systems for Sustainable Design*, M.S. Report, University of South Florida, 2010.

78. “Standard Thermodynamic Properties of Chemical Substances” Update Computer Club [online],
http://www.update.uu.se/~jolkkonen/pdf/CRC_TD.pdf [retrieved 21 January 2014].
79. The Exergoecology Portal [online database],
http://www.exergoecology.com/excalc/index_html/new_calc_exergy [retrieved 21 January 2014].
80. Wall, G., “Exergetics”, Bucamarang, 2009.
81. Green, D.W., Perry, R.H., *Perry’s Chemical Engineers’ Handbook*, 7th ed., Mcgraw-Hill, USA, 1997.
82. “Standard Heats and Free Energies of Formation and Absolute Entropies of Elements and Inorganic Compounds” [online],
<http://wiredchemist.com/chemistry/data/entropies-inorganic> [retrieved 21 January 2014].
83. Exergy calculator [online],
<http://www.exergoecology.com/excalc/exergo/refenv/#equation1> [retrieved 21 January 2014].
84. Sato, N., *Chemical Energy and Exergy, An Introduction to Chemical Thermodynamics for Engineers*, 1st ed., Elsevier, 2004.

APPENDIX A: DATA

Table A.1. Molecular weight and thermodynamical data of the compounds

Chemical compound	MW (g/mol)	ΔH_{f298K}^0 (kJ/mol)	b^0 (kJ/mol)
Glucose	180.16 [67]	-1274.5 [73]	2955 [77]
Oxygen	31.99 [68]	0 [74]	3.97 [78]
H ₂ O ₄ P ⁻	96.99 [69]	-1302.50 [75]	11.32 [79]
NH ₄ ⁺	18.04 [70]	-132.80 [75]	393.14 [79]
Water	18.02 [71]	-285.8 [76]	0.9 [80]
Carbon dioxide	44 [72]	-394 [76]	0
Lipid	1026.6*	-1056 [3]	40,541.8 [3]
Biomass	23.36*	-201.79**	628.15***

**calculated

***calculated via combustion reaction

****calculated via Moran's correlation

APPENDIX B: RESULTS

Table B.1. Parameters of the kinetic models

[NH ₄ ⁺]	t (days)	μ (1/h)	x _{max} (g/L)	x ₀ (g/L)	α _{exp}	β _{exp}
18.7 mM	t ≤ 4	1.0	8.6	1.0x10 ⁻¹	1.0x10 ⁻³	2.0x10 ⁻³
	t > 4	1.0	8.6	1.0x10 ⁻¹	5.0x10 ⁻⁴	-
	t ≥ 6	3.8.0x10 ⁻¹	8.6	1.0x10 ⁻¹	-	-
6.2 mM	t ≤ 1	7.0x10 ⁻¹	6.6	2.5x10 ⁻¹	1.0x10 ⁻³	5.0x10 ⁻⁴
	t > 1	7.0x10 ⁻¹	6.6	2.5x10 ⁻¹	-	-
	t ≥ 6	7.0x10 ⁻¹	6.6	2.5x10 ⁻¹	6.0x10 ⁻⁶	1.8x10 ⁻³
0.7 mM	t ≤ 4	2.4	2.31	1.0x10 ⁻²	5.0x10 ⁻³	2.0x10 ⁻⁴
	t > 4	2.4	2.31	1.0x10 ⁻²	7.4x10 ⁻³	-
	t ≥ 12	2.4	2.31	1.0x10 ⁻²	2.3x10 ⁻²	-
0 mM	t ≤ 11	5.0x10 ⁻²	1.36	8.0x10 ⁻¹	1.5x10 ⁻²	5.0x10 ⁻³
	t > 11	9.5x10 ⁻¹	1.36	8.0x10 ⁻¹	3.0x10 ⁻²	2.0x10 ⁻³

Table B.2. Standard errors of estimate of the kinetic models

[NH ₄ ⁺]	18.7 mM	6.2 mM	0.7 mM	0 mM
SE _{algae growth} (g/L)	2.73x10 ⁻¹	3.79 x10 ⁻¹	8.50x10 ⁻²	2.02x10 ⁻²
SE _{product formation} (g/L)	9.44x10 ⁻⁴	1.49x10 ⁻⁴	5.80x10 ⁻³	7.99x10 ⁻³

Table B.3. Summary of the thermodynamic assessment

[NH ₄ ⁺]	18.7 mM	6.2 mM	0.7 mM	0 mM
Flagellar work (kJ/L)	4.50x10 ⁻⁴	3.55x10 ⁻⁴	1.29x10 ⁻⁴	3.1x10 ⁻⁵
Flagellar work/ (x _{max} - x ₀) (kJ/g)	5.29x10 ⁻⁵	5.59x10 ⁻⁵	5.61x10 ⁻⁵	5.54x10 ⁻⁵
Heat loss (kJ/L)	257.79	203.79	63.86	9.52
Heat loss/(x _{max} - x ₀) (kJ/g)	30.33	32.09	27.76	17
Exergy destruction (kJ/L)	6,286.50	10,512	1,296	453.39
Exergy destruction/ (x _{max} - x ₀) (kJ/g)	739.59	1,655.43	563.48	809.63
Eco-exergy (kJ/L)	6.81	5.52	1.94	1.15
Eco-exergy/ (x _{max} - x ₀) (kJ/g)	8.01x10 ⁻¹	8.69x10 ⁻¹	8.43x10 ⁻¹	2.05
Optical exergy loss (kJ/L)	865.15	682.61	248.92	59.42
Optical exergy loss/ (x _{max} - x ₀) (kJ/g)	101.78	107.50	108.23	106.11
CDP for lipid production (%)	10.24	16.05	15.61	25.55
CDP for biomass production (%)	5.50x10 ⁻¹	7.10x10 ⁻¹	3.40x10 ⁻¹	4.10x10 ⁻¹

APPENDIX C: ALGORITHMS

Algorithm C.1. The algorithm for kinetic analysis for the case where $[\text{NH}_4^+] = 18.7 \text{ mM}$ implemented in MATLAB programming language

```

clear all
close all
format compact
global xmax

% enter the constants

xmax=8.60;

% enter the data
tData1=[0:14];
a=[0 0.10 1.00 2.10 3.20 3.20 3.30 4.18 5.00 5.20 6.20 6.80 7.60
7.70 8.60];
x1=[0; 0.10; 1.00; 2.10; 3.20; 3.20; 3.30; 4.18; 5.00; 5.20;
6.20; 6.80; 7.60; 7.70; 8.60];
lipid=[0 0.0001 0.00325 0.00625 0.00975 0.0121 0.0125 0.0135
0.014 0.0125 0.01525 0.0145 0.014 0.014 0.015];

[t,x]=ode45('odetotalkinetics_first', [0 14], [0.1 0.00000001]);

hold on

[ax, h1, h2]=plotyy(t, x(:,1), t, x(:,2));

set(ax(1), 'ylim', [0 10], 'ytick', [0:1:10], 'ycolor', 'black');
set(ax(2), 'ylim', [0
0.02], 'ytick', [0:0.002:0.02], 'ycolor', 'black');
set(h1, 'LineStyle', ':', 'color', 'black', 'LineWidth', 2);
set(h2, 'LineStyle', '-', 'color', 'black', 'LineWidth', 2);
legend ( 'biomass', 'lipid', 'Location', 'southEast');
[ax, h3, h4]=plotyy(tData1, a, tData1, lipid);
set(h3, 'LineStyle', 'x', 'LineWidth', 2.0, 'Color', 'black');
set(h4, 'LineStyle', 'o', 'LineWidth', 2.0, 'Color', 'black');

```

```

set(get(ax(1), 'Ylabel'), 'String', 'dry biomass (g/L)');
set(get(ax(2), 'Ylabel'), 'String', 'lipid (g/L)');
grid on
xlabel('t(h)')
title ('Kinetic Model - 18.7 mM')
set(ax(1), 'YTick', [0:1:10])
set(ax(1), 'YColor', 'black')
set(ax(2), 'YColor', 'black')

```

Script file

```

function dx = odetotalkinetics_first(t,x);
% This function models product formation with Luedeking-Piret
model
mu=1;
xmax=8.60;

if t<=4;
    mu=0.978;
    xmax=8.6;
    alpha=0.001;
    beta=0.002;
    dx1=mu*x(1)*(1-(x(1)/xmax));
    dx2=alpha*x(1) + beta*dx1;
end

if 4<=t;
    alpha=0.0005;
    beta=0.002;
    dx1=0;
    dx2=alpha*x(1) + beta*dx1;
end

if t>=6;
    mu=0.38;
    xmax=8.6;
    alpha=0.01;
    beta=0.0001;
    dx1=mu*x(1)*(1-(x(1)/xmax));
    dx2=0;
end

```



```
dx = [dx1; dx2];
```

Algorithm C. 2. The algorithm for kinetic analysis for the case where $[\text{NH}_4^+] = 6.2 \text{ mM}$ implemented in MATLAB programming language

M-file

```
clear all
close all
format compact
global mu xmax

% enter the constants
mu=0.7;
xmax=6.6;

% enter the data
tData1=[0:10];
tData2=[0 1 2 3 4 5 6 8 9 10];
a=[0 0.15 1.00 2.0 3.1 4.10 4.42 5.55 5.99 6.27 6.6];
x1=[0; 0.15; 1.00; 2.0; 3.1; 4.10; 4.42; 5.55; 5.99; 6.27; 6.6];
lipid=[0 0.0004 0.0003 0.00041 0.0005 0.0005 0.00049 0.00299
0.00347 0.0036];

[t,x]=ode45('odetotalkinetics_second', [0 10], [0.25 0.00000001])

hold on

[ax, h1, h2]=plotyy(t, x(:,1), t, x(:,2));

set(h1, 'LineStyle', ':', 'color', 'black', 'LineWidth', 2);
set(h2, 'LineStyle', '-', 'color', 'black', 'LineWidth', 2);
legend ('biomass', 'lipid', 'Location', 'SouthEast');
[ax, h3, h4]=plotyy(tData1, a, tData2, lipid);
set(h3, 'LineStyle', '*', 'LineWidth', 2.0, 'Color', 'black');
set(h4, 'LineStyle', 'o', 'LineWidth', 2.0, 'Color', 'black');
set(get(ax(1), 'Ylabel'), 'String', 'dry biomass (g/L)');
grid on
```

```
xlabel('t(h)')  
title('Kinetic Model - 6.2 mM')  
set(ax(1), 'YColor', 'black')  
set(ax(2), 'YColor', 'black')
```

Script file

```
function dx = odetotalkinetics_second(t,x);  
% This function models product formation with Luedeking-Piret  
model  
mu=0.7;  
xmax=6.6;  
  
if t<=1;  
    alpha=0.001;  
    beta=0.0005;  
    dx1=(mu*x(1)*(1-(x(1)/xmax)));  
    dx2=alpha*x(1) + beta*dx1;  
end  
  
if t>1;  
    alpha=0.0001;  
    beta=0.00005;  
    dx1=(mu*x(1)*(1-(x(1)/xmax)));  
    dx2=0;  
end  
  
if t>=6;  
    alpha=0.000006;  
    beta=0.0018;  
    dx1=(mu*x(1)*(1-(x(1)/xmax)));  
    dx2= alpha*x(1) + beta*dx1;  
end  
  
dx=[dx1; dx2];
```

Algorithm C.3. The algorithm for kinetic analysis for the case where $[\text{NH}_4^+] = 0.7 \text{ mM}$ implemented in MATLAB programming language

M-file

```

clear all
close all
format compact
global mu xmax

% enter the constants
mu=2.4;
xmax=2.31;

% enter the data
tData1=[0:14];
a=[0 0.26 1.119 1.92 2.2 2.2 2.18 2.18 2.18 2.29 2.3 2.31 2.31
2.3 2.31];
x1=[0; 0.26; 1.119; 1.92; 2.2; 2.2; 2.18; 2.18; 2.18; 2.29; 2.3;
2.31; 2.31; 2.3; 2.31];
lipid=[0 0 0 0.012 0.02 0.036 0.052 0.0642 0.08 0.094 0.114 0.135
0.158 0.2 0.246];

[t,x]=ode45('odetotalkinetics_third', [0 14], [0.01 0.00004]);

hold on

[ax, h1, h2]=plotyy(t, x(:,1), t, x(:,2));

set(ax(1), 'ylim', [0 2.5], 'ytick', [0:0.5:2.5], 'ycolor', 'black');
set(ax(2), 'ylim', [0
0.25], 'ytick', [0:0.05:0.25], 'ycolor', 'black');
set(h1, 'LineStyle', ':', 'color', 'black', 'LineWidth', 2);
set(h2, 'LineStyle', '-', 'color', 'black', 'LineWidth', 2);
legend ('biomass', 'lipid', 'Location', 'SouthEast');
[ax, h3, h4]=plotyy(tData1, a, tData1, lipid);
set(h3, 'LineStyle', '*', 'LineWidth', 2.0, 'Color', 'black');
set(h4, 'LineStyle', 'o', 'LineWidth', 2.0, 'Color', 'black');
set(get(ax(1), 'Ylabel'), 'String', 'dry biomass (g/L)');
set(get(ax(2), 'Ylabel'), 'String', 'lipid (g/L)');

```

```
grid on
xlabel('t(h)')
title('Kinetic Model - 0.7 mM')
set(ax(1), 'YColor', 'black')
set(ax(2), 'YColor', 'black')
```

Script file

```
function dx= odetotalkinetics_third(t,x);
% This function models substrate consumption
mu=2.4;
xmax=2.31;

if t<=4;
    alpha=0.005;
    beta=0.0002;
    dx1=mu*x(1)*(1-(x(1)/xmax));
    dx2=alpha*x(1) + beta*dx1;
end

if 4<t;
    alpha=0.0074;
    beta=0.0001;
    dx1=0;
    dx2=alpha*x(1);
end

if t>=12;
    alpha=0.023;
    beta=0.001;
    dx1=0;
    dx2=alpha*x(1);
end

dx=[dx1; dx2];
```

Algorithm C.4. The algorithm for kinetic analysis for the case where $[\text{NH}_4^+] = 0 \text{ mM}$ implemented in MATLAB programming language

M-file

```

clear all
close all
format compact
global mu xmax

% enter the constants
mu=0.05;
xmax=1.36;

% enter the data
tData1=[5:14];
a=[0.8 0.86 0.87 0.92 0.98 1.06 1.11 1.24 1.34 1.36];
x1=[0.8; 0.86; 0.87; 0.92; 0.98; 1.06; 1.11; 1.24; 1.34; 1.36];
lipid=[0.0096 0.024 0.0384 0.0456 0.0672 0.0768 0.1056 0.14 0.192
0.2088];

[t,x]=ode45('odetotalkinetics_fourth', [5 14], [0.8 0.0096]);

hold on

[ax, h1, h2]=plotyy(t, x(:,1), t, x(:,2));

set(ax(1), 'ylim', [0 1.5], 'ytick', [0:0.25:1.5], 'ycolor', 'black');
set(ax(2), 'ylim', [0 0.3], 'ytick', [0:0.05:0.3], 'ycolor', 'black');
set(h1, 'LineStyle', ':', 'color', 'black', 'LineWidth', 2);
set(h2, 'LineStyle', '-', 'color', 'black', 'LineWidth', 2);
legend ('biomass', 'lipid', 'Location', 'SouthEast');

[ax, h3, h4]=plotyy(tData1, a, tData1, lipid);
set(h3, 'LineStyle', '*', 'LineWidth', 2.0, 'Color', 'black');
set(h4, 'LineStyle', 'o', 'LineWidth', 2.0, 'Color', 'black');
set(get(ax(1), 'Ylabel'), 'String', 'dry biomass (g/L)');
set(get(ax(2), 'Ylabel'), 'String', 'lipid (g/L)');
grid on
xlabel('t(h)')
title ('Kinetic Model - 0 mM')

```

```
set(ax(1), 'YTick', [0:0.25:1.5])
set(ax(2), 'YTick', [0:0.05:0.3])
set(ax(2), 'YColor', 'black')
set(ax(1), 'YColor', 'black')
```

Script file

```
function dx= odetotalkinetics_fourth(t,x);
% This function models substrate consumption
mu =0.05;
xmax = 1.36;

if t<=11;
    alpha=0.015;
    beta=0.005;
    dx1=mu*x(1);
    dx2=alpha*x(1) + beta*dx1;
end

if t>11;
    mu=0.95;
    alpha=0.03;
    beta=0.002;
    dx1=mu*x(1)*(1-(x(1)/xmax));
    dx2=alpha*x(1) + beta*dx1;
end

dx=[dx1; dx2];
```

Algorithm C.5. The algorithm for work for the case where $[\text{NH}_4^+] = 18.7 \text{ mM}$ implemented in MATLAB programming language

M-file

```
clear all
close all

MW_biomass=23.36;
no_cell=1.3*10^11;
W=(no_cell*1.03*10^(-14))*(-1);

[t,x] = ode45('odetotalkinetics_first', [0 14], [0.1
0.00000001]);

for i=1:60;
    n_biomass(i,:)=((x(i+1,1)-x(i,1))/MW_biomass));
    wb=cumsum(n_biomass*W);
end

for i=1:60;
    time(i)=t(i+1);
end

plot(time, wb, 'k-.', 'LineWidth', 2.0)
xlabel ('t (h)')
ylabel ('Work (kJ/L)')
title ('Flagellar work - 18.7 mM')
grid on
```

Algorithm C.6. The algorithm for work for the case where $[\text{NH}_4^+] = 6.2 \text{ mM}$ implemented in MATLAB programming language

M-file

```

clear all
close all

MW_biomass=23.36;
no_cell=1.3*10^11;
W=(no_cell*1.03*10^(-14))*(-1);

[t,x] = ode45('odetotalkinetics_second', [0 10], [0.25
0.00000001]);

for i=1:60;
    n_biomass(i,:)=((x(i+1,1)-x(i,1))/MW_biomass));
    wb=cumsum(n_biomass*W);
end

for i=1:60;
    time(i)=t(i+1);
end

plot(time, wb, 'k-.', 'LineWidth', 2.0)
xlabel ('t (h)')
ylabel ('Work (kJ/L)')
title ('Flagellar work - 6.2 mM')
grid on

```


Algorithm C.7. The algorithm for work for the case where $[\text{NH}_4^+] = 0.7 \text{ mM}$ implemented in MATLAB programming language

M-file

```
clear all
close all

MW_biomass=23.36;
no_cell=1.3*10^11;
W=(no_cell*1.03*10^(-14))*(-1);

[t,x] = ode45('odetotalkinetics_third', [0 14], [0.01 0.00004]);

for i=1:68;
    n_biomass(i,:)=((x(i+1,1)-x(i,1))/MW_biomass);
    wb=cumsum(n_biomass*W);
end

for i=1:68;
    time(i)=t(i+1);
end

plot(time, wb, 'k-.', 'LineWidth', 2.0)
xlabel ('t (h)')
ylabel ('Work (kJ/L)')
title ('Flagellar work - 0.7 mM')
grid on
```

Algorithm C.8. The algorithm for work for the case where $[\text{NH}_4^+] = 0$ mM implemented in MATLAB programming language

M-file

```
clear all
close all

MW_biomass=23.36;
no_cell=1.3*10^11;
W=(no_cell*1.03*10^(-14))*(-1);

[t,x] = ode45('odetotalkinetics_fourth', [5 14], [0.8 0.0096]);

for i=1:44;
    n_biomass(i,:)=((x(i+1,1)-x(i,1))/MW_biomass);
    wb=cumsum(n_biomass*W);
end

for i=1:44;
    time(i)=t(i+1);
end

plot(time, wb, 'k-.', 'LineWidth', 2.0)
xlabel ('t (h)')
ylabel ('Work (kJ/L)')
title ('Flagellar work - 0 mM')
grid on
```

Algorithm C.9. The algorithm for energy loss for the case where $[\text{NH}_4^+] = 18.7 \text{ mM}$ implemented in MATLAB programming language

M-file

```

clear all
close all

MW_co2=44;
MW_wa=18.02;
MW_o2=31.99;
MW_glu=180.16;
MW_nh=18.04;
MW_hpo=96.99;
MW_biomass=23.36;
MW_tga=1023.6;
T=298;
T0=298;

H_data=[-394; -285.8; 0; -1274.5; -133.26; -1293.01; -201.79; -
1056; 215.9];

[t,x] = ode45('odetotalkinetics_first', [0 14], [0.1
0.00000001]);

% biomass&photosynthesis rxn
for i=1:60;
    n_biomass(i,:)=((x(i+1,1)-x(i,1))/MW_biomass));
    Nh_CO2_BP=n_biomass*4*H_data(1,:);
    Nh_water_BP=n_biomass*3.685*H_data(2,:);
    Nh_nh_BP=n_biomass*0.11*H_data(5,:);
    Nh_hpo_BP=n_biomass*0.01*H_data(6,:);
    Nh_biomass_BP=n_biomass*H_data(7,:);
    Nh_glu_BP=n_biomass*0.5*H_data(4,:);
    Nh_oxygen_BP=n_biomass*4.2125*H_data(3,:);
    Nh_photon=n_biomass*7.353*H_data(9,:);
end

%lipid rxn
for i=1:60;

```

```

n_lipid(i,:)=((x(i+1,2)-x(i,2))/MW_tga));
Nh_glu_TGA=n_lipid*11.5*H_data(4,:);
Nh_oxygen_TGA_in=n_lipid*H_data(3,:);
Nh_lipid_TGA=n_lipid*H_data(8,:);
Nh_oxygen_TGA=n_lipid*22.5*H_data(3,:);
Nh_water_TGA=n_lipid*20*H_data(2,:);
end

% respiration rxn
for i=1:60;
    n_glu_R=((n_biomass*0.5)-(n_lipid*11.5));
    Nh_glu_R=n_glu_R*H_data(4,:);
    Nh_oxygen_R=n_glu_R*6*H_data(3,:);
    Nh_CO2_R=n_glu_R*6*H_data(1,:);
    Nh_water_R=n_glu_R*6*H_data(2,:);
end

for i=60;
    Nh_oxygen_ex=((n_biomass*4.2125)-(n_lipid*22.5)-
        (n_glu_R*6))*H_data(3,:);
    Nb_oxygen_ex=((n_biomass*4.2125)-(n_lipid*22.5)-
        (n_glu_R*6))*b_data(3,:);
end

Qin=Nh_CO2_BP+Nh_water_BP+Nh_nh_BP+Nh_hpo_BP+Nh_photon;
Qout=Nh_CO2_R+Nh_water_R+Nh_oxygen_TGA+Nh_water_TGA+Nh_oxygen_ex;
Qacc=Nh_lipid_TGA+Nh_biomass_BP;
Q_total=cumsum((Qout-Qin-Qacc));

for i=1:60;
    time(i)=t(i+1);
end

plot(time, Q_total, 'k-.', 'LineWidth', 2.0)
xlabel ('t (h)')
ylabel ('Q (kJ/L)')
title ('Energy loss - 18.7 mM')
grid on

```

Algorithm C.10. The algorithm for energy loss for the case where $[\text{NH}_4^+] = 6.2 \text{ mM}$ implemented in MATLAB programming language

M-file

```
clear all
close all

MW_co2=44;
MW_wa=18.02;
MW_o2=31.99;
MW_glu=180.16;
MW_nh=18.04;
MW_hpo=96.99;
MW_biomass=23.36;
MW_tga=1023.6;
T=298;
T0=298;

H_data=[-394; -285.8; 0; -1274.5; -133.26; -1293.01; -201.79; -
1056; 215.9];

[t,x] = ode45('odetotalkinetics_second', [0 10], [0.25
0.00000001]);

% biomass&photosynthesis rxn
for i=1:60;
    n_biomass(i,:) = ((x(i+1,1) - x(i,1)) / MW_biomass);
    Nh_CO2_BP = n_biomass * 4 * H_data(1,:);
    Nh_water_BP = n_biomass * 3.685 * H_data(2,:);
    Nh_nh_BP = n_biomass * 0.11 * H_data(5,:);
    Nh_hpo_BP = n_biomass * 0.01 * H_data(6,:);
    Nh_biomass_BP = n_biomass * H_data(7,:);
    Nh_glu_BP = n_biomass * 0.5 * H_data(4,:);
    Nh_oxygen_BP = n_biomass * 4.2125 * H_data(3,:);
    Nh_photon = n_biomass * 7.353 * H_data(9,:);
end

%lipid rxn
for i=1:60;
```

```

n_lipid(i,:)=((x(i+1,2)-x(i,2))/MW_tga));
Nh_glu_TGA=n_lipid*11.5*H_data(4,:);
Nh_oxygen_TGA_in=n_lipid*H_data(3,:);
Nh_lipid_TGA=n_lipid*H_data(8,:);
Nh_oxygen_TGA=n_lipid*22.5*H_data(3,:);
Nh_water_TGA=n_lipid*20*H_data(2,:);
end

% respiration rxn
for i=1:60;
    n_glu_R=((n_biomass*0.5)-(n_lipid*11.5));
    Nh_glu_R=n_glu_R*H_data(4,:);
    Nh_oxygen_R=n_glu_R*6*H_data(3,:);
    Nh_CO2_R=n_glu_R*6*H_data(1,:);
    Nh_water_R=n_glu_R*6*H_data(2,:);
end

for i=60;
    Nh_oxygen_ex=((n_biomass*4.2125)-(n_lipid*22.5)-
        (n_glu_R*6))*H_data(3,:);
    Nb_oxygen_ex=((n_biomass*4.2125)-(n_lipid*22.5)-
        (n_glu_R*6))*b_data(3,:);
end

Qin=Nh_CO2_BP+Nh_water_BP+Nh_nh_BP+Nh_hpo_BP+Nh_photon;
Qout=Nh_CO2_R+Nh_water_R+Nh_oxygen_TGA+Nh_water_TGA+Nh_oxygen_ex;
Qacc=Nh_lipid_TGA+Nh_biomass_BP;
Q_total=cumsum((Qout-Qin-Qacc));

for i=1:60;
    time(i)=t(i+1);
end

plot(time, Q_total, 'k-.', 'LineWidth', 2.0)
xlabel ('t (h)')
ylabel ('Q (kJ/L)')
title ('Energy loss - 6.2 mM')
grid on

```

Algorithm C.11. The algorithm for energy loss for the case where $[\text{NH}_4^+] = 0.7 \text{ mM}$ implemented in MATLAB programming language

M-file

```

clear all
close all

MW_co2=44;
MW_wa=18.02;
MW_o2=31.99;
MW_glu=180.16;
MW_nh=18.04;
MW_hpo=96.99;
MW_biomass=23.36;
MW_tga=1023.6;
T=298;
T0=298;

H_data=[-394; -285.8; 0; -1274.5; -133.26; -1293.01; -201.79; -
1056; 215.9];

[t,x] = ode45('odetotalkinetics_third', [0 14], [0.01 0.00004]);

% biomass&photosynthesis rxn
for i=1:68;
    n_biomass(i,:)=((x(i+1,1)-x(i,1))/MW_biomass));
    Nh_CO2_BP=n_biomass*4*H_data(1,:);
    Nh_water_BP=n_biomass*3.685*H_data(2,:);
    Nh_nh_BP=n_biomass*0.11*H_data(5,:);
    Nh_hpo_BP=n_biomass*0.01*H_data(6,:);
    Nh_biomass_BP=n_biomass*H_data(7,:);
    Nh_glu_BP=n_biomass*0.5*H_data(4,:);
    Nh_oxygen_BP=n_biomass*4.2125*H_data(3,:);
    Nh_photon=n_biomass*7.353*H_data(9,:);
end

%lipid rxn
for i=1:68;
    n_lipid(i,:)=((x(i+1,2)-x(i,2))/MW_tga));

```

```

    Nh_glu_TGA=n_lipid*11.5*H_data(4,:);
    Nh_oxygen_TGA_in=n_lipid*H_data(3,:);
    Nh_lipid_TGA=n_lipid*H_data(8,:);
    Nh_oxygen_TGA=n_lipid*22.5*H_data(3,:);
    Nh_water_TGA=n_lipid*20*H_data(2,:);
end

% respiration rxn
for i=1:68;
    n_glu_R=((n_biomass*0.5)-(n_lipid*11.5));
    Nh_glu_R=n_glu_R*H_data(4,:);
    Nh_oxygen_R=n_glu_R*6*H_data(3,:);
    Nh_CO2_R=n_glu_R*6*H_data(1,:);
    Nh_water_R=n_glu_R*6*H_data(2,:);
end

for i=68;
    Nh_oxygen_ex=((n_biomass*4.2125)-(n_lipid*22.5)-
        (n_glu_R*6))*H_data(3,:);
    Nb_oxygen_ex=((n_biomass*4.2125)-(n_lipid*22.5)-
        (n_glu_R*6))*b_data(3,:);
end

Qin=Nh_CO2_BP+Nh_water_BP+Nh_nh_BP+Nh_hpo_BP+Nh_photon;
Qout=Nh_CO2_R+Nh_water_R+Nh_oxygen_TGA+Nh_water_TGA+Nh_oxygen_ex;
Qacc=Nh_lipid_TGA+Nh_biomass_BP;
Q_total=cumsum((Qout-Qin-Qacc));

for i=1:68;
    time(i)=t(i+1);
end

plot(time, Q_total, 'k-.', 'LineWidth', 2.0)
xlabel ('t (h)')
ylabel ('Q (kJ/L)')
title ('Energy loss - 0.7 mM')
grid on

```


Algorithm C.12. The algorithm for energy loss for the case where $[\text{NH}_4^+] = 0 \text{ mM}$ implemented in MATLAB programming language

M-file

```

clear all
close all

MW_co2=44;
MW_wa=18.02;
MW_o2=31.99;
MW_glu=180.16;
MW_nh=18.04;
MW_hpo=96.99;
MW_biomass=23.36;
MW_tga=1023.6;
T=298;
T0=298;

H_data=[-394; -285.8; 0; -1274.5; -133.26; -1293.01; -201.79; -
1056; 215.9];

[t,x] = ode45('odetotalkinetics_fourth', [5 14], [0.8 0.0096]);

% biomass&photosynthesis rxn
for i=1:44;
    n_biomass(i,:)=((x(i+1,1)-x(i,1))/MW_biomass));
    Nh_CO2_BP=n_biomass*4*H_data(1,:);
    Nh_water_BP=n_biomass*3.685*H_data(2,:);
    Nh_nh_BP=n_biomass*0.11*H_data(5,:);
    Nh_hpo_BP=n_biomass*0.01*H_data(6,:);
    Nh_biomass_BP=n_biomass*H_data(7,:);
    Nh_glu_BP=n_biomass*0.5*H_data(4,:);
    Nh_oxygen_BP=n_biomass*4.2125*H_data(3,:);
    Nh_photon=n_biomass*7.353*H_data(9,:);
end

%lipid rxn
for i=1:44;
    n_lipid(i,:)=((x(i+1,2)-x(i,2))/MW_tga));

```

```

    Nh_glu_TGA=n_lipid*11.5*H_data(4,:);
    Nh_oxygen_TGA_in=n_lipid*H_data(3,:);
    Nh_lipid_TGA=n_lipid*H_data(8,:);
    Nh_oxygen_TGA=n_lipid*22.5*H_data(3,:);
    Nh_water_TGA=n_lipid*20*H_data(2,:);
end

% respiration rxn
for i=1:44;
    n_glu_R=(n_biomass*0.5)-(n_lipid*11.5);
    Nh_glu_R=n_glu_R*H_data(4,:);
    Nh_oxygen_R=n_glu_R*6*H_data(3,:);
    Nh_CO2_R=n_glu_R*6*H_data(1,:);
    Nh_water_R=n_glu_R*6*H_data(2,:);
end

for i=44;
    Nh_oxygen_ex=((n_biomass*4.2125)-(n_lipid*22.5)-
        (n_glu_R*6))*H_data(3,:);
    Nb_oxygen_ex=((n_biomass*4.2125)-(n_lipid*22.5)-
        (n_glu_R*6))*b_data(3,:);
end

Qin=Nh_CO2_BP+Nh_water_BP+Nh_nh_BP+Nh_hpo_BP+Nh_photon;
Qout=Nh_CO2_R+Nh_water_R+Nh_oxygen_TGA+Nh_water_TGA+Nh_oxygen_ex;
Qacc=Nh_lipid_TGA+Nh_biomass_BP;
Q_total=cumsum((Qout-Qin-Qacc));

for i=1:44;
    time(i)=t(i+1);
end

plot(time, Q_total, 'k-.', 'LineWidth', 2.0)
xlabel ('t (h)')
ylabel ('Q (kJ/L)')
title ('Energy loss - 0 mM')
grid on

```

Algorithm C.13. The algorithm for exergy destruction for the case where $[\text{NH}_4^+] = 18.7 \text{ mM}$ implemented in MATLAB programming language

M-file

```
clear all
close all

MW_co2=44;
MW_wa=18.02;
MW_o2=31.99;
MW_glu=180.16;
MW_nh=18.04;
MW_hpo=96.99;
MW_biomass=23.36;
MW_tga=1023.6;
R=0.008314;
T=298;
T0=298;

b_data=[0; 0.9; 3.97; 2955; 393.14; 11.32;628.15; 40541.751;
2577.5];

[t,x] = ode45('odetotalkinetics_first', [0 14], [0.1
0.00000001]);

%ex inlet

n_biomass=x(:,1)/MW_biomass;
n_co2_in=n_biomass*4;
n_water_in=n_biomass*3.685;
n_nh_in=n_biomass*0.11;
n_hpo_in=n_biomass*0.01;
n_photon_in=n_biomass*7.353;
n_in_total=n_biomass+
n_co2_in+n_water_in+n_nh_in+n_hpo_in+n_photon_in;

y_co2_in=n_co2_in./n_in_total;
y_water_in=n_water_in./n_in_total;
y_nh_in=n_nh_in./n_in_total;
```

```

y_hpo_in=n_hpo_in./n_in_total;

b_co2_in=(log(y_co2_in))*R*T+b_data(1, :)*n_co2_in;
b_water_in=(log(y_water_in))*R*T+b_data(2, :)*n_water_in;
b_nh_in=(log(y_nh_in))*R*T+b_data(5, :)*n_nh_in;
b_hpo_in=(log(y_hpo_in))*R*T+b_data(6, :)*n_hpo_in;

%ex out

n_biomass=x(:,1)/MW_biomass;
n_lipid=x(:,2)/MW_tga;
n_co2_out=((n_biomass*0.5)-(n_lipid*11.5))*6;
n_o2_out=(n_biomass*4.2125)-(n_lipid)-(((n_biomass*0.5)-
(n_lipid*11.5))*6)+(n_lipid*22.5);
n_h2o_out=(n_lipid*20)+((n_biomass*0.5)-(n_lipid*11.5))*6;
n_out_total=n_co2_out+n_o2_out+ n_h2o_out;

y_co2_out=n_co2_out./n_out_total;
y_o2_out=n_o2_out./n_out_total;
y_h2o_out=n_h2o_out./n_out_total;

b_co2_out=(log(y_co2_out))*R*T+b_data(1, :)*n_co2_out;
b_o2_out=(log(y_o2_out))*R*T+b_data(3, :)*n_o2_out;
b_h2o_out=(log(y_h2o_out))*R*T+b_data(2, :)*n_h2o_out;

%ex acc

n_glu=n_biomass*0.5;
n_o2=n_biomass*4.2125;
n_acc_total=n_biomass+n_lipid+n_glu+n_o2-n_o2_out;

y_biomass=n_biomass./n_acc_total;
y_lipid=n_lipid./n_acc_total;
y_glu=n_glu./ n_acc_total;
y_o2=n_o2./ n_acc_total;

b_biomass_acc=(log(y_biomass))*R*T+b_data(7, :)*n_biomass;
b_lipid_acc=(log(y_lipid))*R*T+b_data(8, :)*n_lipid;
b_glu=log(y_glu)*R*T+b_data(4, :)*n_glu;
b_o2=log(y_o2)*R*T+b_data(3, :)*n_o2;

```

```

Nbin=(b_co2_in.*n_co2_in+( b_water_in.*n_water_in)+(
b_nh_in.*n_nh_in)+(b_hpo_in.*n_hpo_in)+(b_data(9,:).*n_photon_in)
);
Nbout=(b_co2_out.*n_co2_out)+(b_o2_out.*n_o2_out)+(b_h2o_out.*n_h
2o_out);
Nbacc=(b_biomass_acc.*n_biomass)+(b_lipid_acc.*n_lipid)+(b_glu.*n
_glu)+(b_o2.*n_o2-b_o2_out.*n_o2_out);
deltab=Nbin-Nbout-Nbacc;
Xdestroyed=cumsum(deltab);

for i=1:60;
    Xdestroyed_C(i,:)=Xdestroyed(i+1,:)-Xdestroyed(i,:);
end

for i=1:60;
    time(i)=t(i+1);
end

plot(time,Xdestroyed_C, 'k-.', 'LineWidth', 2.0)
xlabel ('t (h)')
ylabel ('Xdestroyed (kJ/L)')
title ('Exergy Destruction - 18.7 mM')
grid on

```

Algorithm C.14. The algorithm for exergy destruction for the case where $[\text{NH}_4^+] = 6.2 \text{ mM}$ implemented in MATLAB programming language

M-file

```

clear all
close all

MW_co2=44;
MW_wa=18.02;
MW_o2=31.99;
MW_glu=180.16;
MW_nh=18.04;

```

```

MW_hpo=96.99;
MW_biomass=23.36;
MW_tga=1023.6;
R=0.008314;
T=298;
T0=298;

b_data=[0; 0.9; 3.97; 2955; 393.14; 11.32;628.15; 40541.751;
2577.5];

[t,x] = ode45('odetotalkinetics_second', [0 10], [0.25
0.00000001]);

%ex inlet

n_biomass=x(:,1)/MW_biomass;
n_co2_in=n_biomass*4;
n_water_in=n_biomass*3.685;
n_nh_in=n_biomass*0.11;
n_hpo_in=n_biomass*0.01;
n_photon_in=n_biomass*7.353;
n_in_total=n_biomass+
n_co2_in+n_water_in+n_nh_in+n_hpo_in+n_photon_in;

y_co2_in=n_co2_in./n_in_total;
y_water_in=n_water_in./n_in_total;
y_nh_in=n_nh_in./n_in_total;
y_hpo_in=n_hpo_in./n_in_total;

b_co2_in=(log(y_co2_in)*R*T+b_data(1,:)*n_co2_in);
b_water_in=(log(y_water_in))*R*T+b_data(2,:)*n_water_in;
b_nh_in=(log(y_nh_in))*R*T+b_data(5,:)*n_nh_in;
b_hpo_in=(log(y_hpo_in))*R*T+b_data(6,:)+n_hpo_in;

%ex out

n_biomass=x(:,1)/MW_biomass;
n_lipid=x(:,2)/MW_tga;
n_co2_out=((n_biomass*0.5)-(n_lipid*11.5))*6);

```

```

n_o2_out=(n_biomass*4.2125)-(n_lipid)-(((n_biomass*0.5)-
(n_lipid*11.5))*6)+(n_lipid*22.5);
n_h2o_out=(n_lipid*20)+(((n_biomass*0.5)-(n_lipid*11.5))*6);
n_out_total=n_co2_out+n_o2_out+ n_h2o_out;

y_co2_out=n_co2_out./n_out_total;
y_o2_out=n_o2_out./n_out_total;
y_h2o_out=n_h2o_out./n_out_total;

b_co2_out=(log(y_co2_out))*R*T+b_data(1, :)*n_co2_out;
b_o2_out=(log(y_o2_out))*R*T+b_data(3, :)*n_o2_out;
b_h2o_out=(log(y_h2o_out))*R*T+b_data(2, :)*n_h2o_out;

%ex acc
n_glu=n_biomass*0.5;
n_o2=n_biomass*4.2125;
n_acc_total=n_biomass+n_lipid+n_glu+n_o2-n_o2_out;

y_biomass=n_biomass./n_acc_total;
y_lipid=n_lipid./n_acc_total;
y_glu=n_glu./ n_acc_total;
y_o2=n_o2./ n_acc_total;

b_biomass_acc=(log(y_biomass))*R*T+b_data(7, :)*n_biomass;
b_lipid_acc=(log(y_lipid))*R*T+b_data(8, :)*n_lipid;
b_glu=log(y_glu)*R*T+b_data(4, :)*n_glu;
b_o2=log(y_o2)*R*T+b_data(3, :)*n_o2;

Nbin=(b_co2_in.*n_co2_in+( b_water_in.*n_water_in)+(
b_nh_in.*n_nh_in)+(b_hpo_in.*n_hpo_in)+(b_data(9, :).*n_photon_in)
);
Nbout=(b_co2_out.*n_co2_out)+(b_o2_out.*n_o2_out)+(b_h2o_out.*n_h
2o_out);
Nbacc=(b_biomass_acc.*n_biomass)+(b_lipid_acc.*n_lipid)+(b_glu.*n
_glu)+(b_o2.*n_o2-b_o2_out.*n_o2_out);
deltab=Nbin-Nbout-Nbacc;
Xdestroyed=cumsum(deltab);

for i=1:60;

```

```

        Xdestroyed_C(i,:)=Xdestroyed(i+1,:)-Xdestroyed(i,:);
end

for i=1:60;
    time(i)=t(i+1);
end

plot(time,Xdestroyed_C, 'k-.', 'LineWidth', 2.0)
xlabel ('t (h)')
ylabel ('Xdestroyed (kJ/L)')
title ('Exergy Destruction - 6.2 mM')
grid on

```

Algorithm C.15. The algorithm for exergy destruction for the case where $[\text{NH}_4^+] = 0.7 \text{ mM}$ implemented in MATLAB programming language

M-file

```

clear all
close all

MW_co2=44;
MW_wa=18.02;
MW_o2=31.99;
MW_glu=180.16;
MW_nh=18.04;
MW_hpo=96.99;
MW_biomass=23.36;
MW_tga=1023.6;
R=0.008314;
T=298;
T0=298;

b_data=[0; 0.9; 3.97; 2955; 393.14; 11.32;628.15; 40541.751;
2577.5];

[t,x] = ode45('odetotalkinetics_third', [0 14], [0.01 0.00004]);

%ex inlet

```



```

n_biomass=x(:,1)/MW_biomass;
n_co2_in=n_biomass*4;
n_water_in=n_biomass*3.685;
n_nh_in=n_biomass*0.11;
n_hpo_in=n_biomass*0.01;
n_photon_in=n_biomass*7.353;

n_in_total=n_biomass+n_co2_in+n_water_in+n_nh_in+n_hpo_in+n_p
hoton_in;

y_co2_in=n_co2_in./n_in_total;
y_water_in=n_water_in./n_in_total;
y_nh_in=n_nh_in./n_in_total;
y_hpo_in=n_hpo_in./n_in_total;

b_co2_in=(log(y_co2_in))*R*T+b_data(1,:)*n_co2_in;
b_water_in=(log(y_water_in))*R*T+b_data(2,:)*n_water_in;
b_nh_in=(log(y_nh_in))*R*T+b_data(5,:)*n_nh_in;
b_hpo_in=(log(y_hpo_in))*R*T+b_data(6,:)+n_hpo_in;

%ex out

n_biomass=x(:,1)/MW_biomass;
n_lipid=x(:,2)/MW_tga;
n_co2_out=((n_biomass*0.5)-(n_lipid*11.5))*6;
n_o2_out=(n_biomass*4.2125)-(n_lipid)-(((n_biomass*0.5)-
(n_lipid*11.5))*6)+(n_lipid*22.5);
n_h2o_out=(n_lipid*20)+(((n_biomass*0.5)-(n_lipid*11.5))*6);
n_out_total=n_co2_out+n_o2_out+ n_h2o_out;

y_co2_out=n_co2_out./n_out_total;
y_o2_out=n_o2_out./n_out_total;
y_h2o_out=n_h2o_out./n_out_total;

b_co2_out=(log(y_co2_out))*R*T+b_data(1,:)*n_co2_out;
b_o2_out=(log(y_o2_out))*R*T+b_data(3,:)*n_o2_out;
b_h2o_out=(log(y_h2o_out))*R*T+b_data(2,:)*n_h2o_out;

```

```

%ex acc
    n_glu=n_biomass*0.5;
    n_o2=n_biomass*4.2125;
    n_acc_total=n_biomass+n_lipid+n_glu+n_o2-n_o2_out;

    y_biomass=n_biomass./n_acc_total;
    y_lipid=n_lipid./n_acc_total;
    y_glu=n_glu./ n_acc_total;
    y_o2=n_o2./ n_acc_total;

    b_biomass_acc=(log(y_biomass))*R*T+b_data(7,:)*n_biomass;
    b_lipid_acc=(log(y_lipid))*R*T+b_data(8,:)*n_lipid;
    b_glu=log(y_glu)*R*T+b_data(4,:)*n_glu;
    b_o2=log(y_o2)*R*T+b_data(3,:)*n_o2;

Nbin=(b_co2_in.*n_co2_in+( b_water_in.*n_water_in)+(
b_nh_in.*n_nh_in)+(b_hpo_in.*n_hpo_in)+(b_data(9,:).*n_photon_in
));
Nbout=(b_co2_out.*n_co2_out)+(b_o2_out.*n_o2_out)+(b_h2o_out.*n_h
2o_out);
Nbacc=(b_biomass_acc.*n_biomass)+(b_lipid_acc.*n_lipid)+(b_glu.*n
_glu)+(b_o2.*n_o2-b_o2_out.*n_o2_out);
deltab=Nbin-Nbout-Nbacc;
Xdestroyed=cumsum(deltab);

for i=1:68;
    Xdestroyed_C(i,:)=Xdestroyed(i+1,:)-Xdestroyed(i,:);
end

for i=1:68;
    time(i)=t(i+1);
end

plot(time,Xdestroyed_C, 'k-.', 'LineWidth', 2.0)
xlabel ('t (h)')
ylabel ('Xdestroyed (kJ/L)')
title ('Exergy Destruction - 0.7 mM')
grid on

```

Algorithm C.16. The algorithm for exergy destruction for the case where $[\text{NH}_4^+] = 0 \text{ mM}$ implemented in MATLAB programming language

M-file

```
clear all
close all

MW_co2=44;
MW_wa=18.02;
MW_o2=31.99;
MW_glu=180.16;
MW_nh=18.04;
MW_hpo=96.99;
MW_biomass=23.36;
MW_tga=1023.6;
R=0.008314;
T=298;
T0=298;

b_data=[0; 0.9; 3.97; 2955; 393.14; 11.32;628.15; 40541.751;
2577.5];

[t,x] = ode45('odetotalkinetics_fourth', [5 14], [0.8 0.0096]);

%ex inlet

n_biomass=x(:,1)/MW_biomass;
n_co2_in=n_biomass*4;
n_water_in=n_biomass*3.685;
n_nh_in=n_biomass*0.11;
n_hpo_in=n_biomass*0.01;
n_photon_in=n_biomass*7.353;

n_in_total=n_biomass+n_co2_in+n_water_in+n_nh_in+n_hpo_in+n_p
hoton_in;

y_co2_in=n_co2_in./n_in_total;
y_water_in=n_water_in./n_in_total;
y_nh_in=n_nh_in./n_in_total;
```

```

y_hpo_in=n_hpo_in./n_in_total;

b_co2_in=(log(y_co2_in))*R*T+b_data(1, :)*n_co2_in;
b_water_in=(log(y_water_in))*R*T+b_data(2, :)*n_water_in;
b_nh_in=(log(y_nh_in))*R*T+b_data(5, :)*n_nh_in;
b_hpo_in=(log(y_hpo_in))*R*T+b_data(6, :)*n_hpo_in;

%ex out

n_biomass=x(:,1)/MW_biomass;
n_lipid=x(:,2)/MW_tga;
n_co2_out=((n_biomass*0.5)-(n_lipid*11.5))*6;
n_o2_out=(n_biomass*4.2125)-(n_lipid)-(((n_biomass*0.5)-
(n_lipid*11.5))*6)+(n_lipid*22.5);
n_h2o_out=(n_lipid*20)+((n_biomass*0.5)-(n_lipid*11.5))*6;
n_out_total=n_co2_out+n_o2_out+ n_h2o_out;

y_co2_out=n_co2_out./n_out_total;
y_o2_out=n_o2_out./n_out_total;
y_h2o_out=n_h2o_out./n_out_total;

b_co2_out=(log(y_co2_out))*R*T+b_data(1, :)*n_co2_out;
b_o2_out=(log(y_o2_out))*R*T+b_data(3, :)*n_o2_out;
b_h2o_out=(log(y_h2o_out))*R*T+b_data(2, :)*n_h2o_out;

%ex acc

n_glu=n_biomass*0.5;
n_o2=n_biomass*4.2125;
n_acc_total=n_biomass+n_lipid+n_glu+n_o2-n_o2_out;

y_biomass=n_biomass./n_acc_total;
y_lipid=n_lipid./n_acc_total;
y_glu=n_glu./ n_acc_total;
y_o2=n_o2./ n_acc_total;

b_biomass_acc=(log(y_biomass))*R*T+b_data(7, :)*n_biomass;
b_lipid_acc=(log(y_lipid))*R*T+b_data(8, :)*n_lipid;
b_glu=log(y_glu)*R*T+b_data(4, :)*n_glu;
b_o2=log(y_o2)*R*T+b_data(3, :)*n_o2;

```

```

Nbin=(b_co2_in.*n_co2_in+( b_water_in.*n_water_in)+(
b_nh_in.*n_nh_in)+(b_hpo_in.*n_hpo_in)+(b_data(9,:).*n_photon_in)
);
Nbout=(b_co2_out.*n_co2_out)+(b_o2_out.*n_o2_out)+(b_h2o_out.*n_h
2o_out);
Nbacc=(b_biomass_acc.*n_biomass)+(b_lipid_acc.*n_lipid)+(b_glu.*n
_glu)+(b_o2.*n_o2-b_o2_out.*n_o2_out);
deltab=Nbin-Nbout-Nbacc;
Xdestroyed=cumsum(deltab);

for i=1:44;
    Xdestroyed_C(i,:)=Xdestroyed(i+1,:)-Xdestroyed(i,:);
end

for i=1:44;
    time(i)=t(i+1);
end

plot(time,Xdestroyed_C, 'k-.', 'LineWidth', 2.0)
xlabel ('t (h)')
ylabel ('Xdestroyed (kJ/L)')
title ('Exergy Destruction - 0 mM')
grid on

```

Algorithm C.17. The algorithm for eco-exergy for the case where $[\text{NH}_4^+] = 18.7 \text{ mM}$ implemented in MATLAB programming language

M-file

```

clear all
close all

MW_biomass=23.36;
beta=20;

b_data=[0; 0.9; 3.97; 2955; 393.14; 11.32;628.15; 40541.751;
2577.5];

```

```

[t,x] = ode45('odetotalkinetics_first', [0 14], [0.1
0.00000001]);

n_biomass=x(:,1)/MW_biomass;
eco=cumsum(n_biomass*beta);

for i=1:60;
    eco_c(i,:)=eco(i+1,:)-eco(i,:);
end

for i=1:60;
    time(i)=t(i+1);
end

plot(time, eco_c, 'k-.', 'LineWidth', 2.0)
xlabel ('t (h)')
ylabel ('Eco-exergy (kJ/L)')
title ('Eco-exergy - 18.7 mM')
grid on

```

Algorithm C.18. The algorithm for eco-exergy for the case where $[\text{NH}_4^+] = 6.2 \text{ mM}$ implemented in MATLAB programming language

M-file

```

clear all
close all

MW_biomass=23.36;
beta=20;

b_data=[0; 0.9; 3.97; 2955; 393.14; 11.32;628.15; 40541.751;
2577.5];

[t,x] = ode45('odetotalkinetics_second', [0 10], [0.25
0.00000001]);

n_biomass=x(:,1)/MW_biomass;

```

```

eco=cumsum(n_biomass*beta);

for i=1:60;
    eco_c(i,:)=eco(i+1,:)-eco(i,:);
end

for i=1:60;
    time(i)=t(i+1);
end

plot(time, eco_c, 'k-.', 'LineWidth', 2.0)
xlabel ('t (h)')
ylabel ('Eco-exergy (kJ/L)')
title ('Eco-exergy - 6.2 mM')
grid on

```

Algorithm C.19. The algorithm for eco-exergy for the case where $[\text{NH}_4^+] = 0.7 \text{ mM}$ implemented in MATLAB programming language

M-file

```

clear all
close all

MW_biomass=23.36;
beta=20;

b_data=[0; 0.9; 3.97; 2955; 393.14; 11.32;628.15; 40541.751;
2577.5];

[t,x] = ode45('odetotalkinetics_third', [0 14], [0.01 0.00004]);

n_biomass=x(:,1)/MW_biomass;
eco=cumsum(n_biomass*beta);

for i=1:68;
    eco_c(i,:)=eco(i+1,:)-eco(i,:);
end

```

```

for i=1:68;
    time(i)=t(i+1);
end

plot(time, eco_c, 'k-.', 'LineWidth', 2.0)
xlabel ('t (h)')
ylabel ('Eco-exergy (kJ/L)')
title ('Eco-exergy - 0.7 mM')
grid on

```

Algorithm C.20. The algorithm for eco-exergy for the case where $[\text{NH}_4^+] = 0 \text{ mM}$ implemented in MATLAB programming language

M-file

```

clear all
close all

MW_biomass=23.36;
beta=20;

b_data=[0; 0.9; 3.97; 2955; 393.14; 11.32;628.15; 40541.751;
2577.5];

[t,x] = ode45('odetotalkinetics_fourth', [5 14], [0.8 0.0096]);

n_biomass=x(:,1)/MW_biomass;
eco=cumsum(n_biomass*beta);

for i=1:44;
    eco_c(i,:)=eco(i+1,:)-eco(i,:);
end

for i=1:44;
    time(i)=t(i+1);
end

plot(time, eco_c, 'k-.', 'LineWidth', 2.0)
xlabel ('t (h)')

```



```

ylabel ('Eco-exergy (kJ/L)')
title ('Eco-exergy - 0 mM')
grid on

```

Algorithm C. 21. The algorithm for optical exergy loss for the case where $[\text{NH}_4^+] = 18.7 \text{ mM}$ implemented in MATLAB programming language

```

M-file

clear all
close all

MW_biomass=23.36;
l=17.9;
e=37.93;
ex_photon=2577.5;

[t,x] = ode45('odetotalkinetics_first', [0 14], [0.1
0.00000001]);

for i=1:60;
    n_biomass(i,:)=(x(i+1,1)-x(i,1))/MW_biomass;
    A=cumsum(n_biomass*e*l);
    Azero=e*0.0006*l;
    fraction=1-(Azero/A);
    Exergy_source=cumsum(n_biomass*ex_photon*fraction);
end

for i=1:60;
    time(i)=t(i+1);
end

plot(time, Exergy_source, 'k', 'Linewidth', 2)
xlabel ('t (h)')
ylabel ('Xdestroyed-optical (kJ/L)')
title ('Optical Exergy Loss - 18.7 mM')
grid on

```

Algorithm C.22. The algorithm for optical exergy loss for the case where $[\text{NH}_4^+] = 6.2 \text{ mM}$ implemented in MATLAB programming language

M-file

```
clear all
close all

MW_biomass=23.36;
l=17.9;
e=37.93;
ex_photon=2577.5;

[t,x] = ode45('odetotalkinetics_second', [0 10], [0.25
0.00000001]);

for i=1:60;
    n_biomass(i,:)=(x(i+1,1)-x(i,1))/MW_biomass;
    A=cumsum(n_biomass*e*l);
    Azero=e*0.0006*l;
    fraction=1-(Azero/A);
    Exergy_source=cumsum(n_biomass*ex_photon*fraction);
end

for i=1:60;
    time(i)=t(i+1);
end

plot(time, Exergy_source, 'k', 'Linewidth', 2)
xlabel ('t (h)')
ylabel ('Xdestroyed-optical (kJ/L)')
title ('Optical Exergy Loss - 6.2 mM')
grid on
```

Algorithm C.23. The algorithm for optical exergy loss for the case where $[\text{NH}_4^+] = 0.7 \text{ mM}$ implemented in MATLAB programming language

M-file

```
clear all
close all

MW_biomass=23.36;
l=17.9;
e=37.93;
ex_photon=2577.5;

[t,x] = ode45('odetotalkinetics_third', [0 14], [0.01 0.00004]);

for i=1:68;
    n_biomass(i,:)=((x(i+1,1)-x(i,1))/MW_biomass);
    A=cumsum(n_biomass*e*l);
    Azero=e*0.0006*l;
    fraction=1-(Azero/A);
    Exergy_source=cumsum(n_biomass*ex_photon*fraction);
end

for i=1:68;
    time(i)=t(i+1);
end

plot(time, Exergy_source, 'k', 'Linewidth', 2)
xlabel ('t (h)')
ylabel ('Xdestroyed-optical (kJ/L)')
title ('Optical Exergy Loss - 0.7 mM')
grid on
```

Algorithm C.24. The algorithm for optical exergy loss for the case where $[\text{NH}_4^+] = 0 \text{ mM}$ implemented in MATLAB programming language

M-file

```
clear all
close all

MW_biomass=23.36;
l=17.9;
e=37.93;
ex_photon=2577.5;

[t,x] = ode45('odetotalkinetics_fourth', [5 14], [0.8 0.0096]);

for i=1:44;
    n_biomass(i,:)=((x(i+1,1)-x(i,1))/MW_biomass);
    A=cumsum(n_biomass*e*l);
    Azero=e*0.0006*l;
    fraction=1-(Azero/A);
    Exergy_source=cumsum(n_biomass*ex_photon*fraction);
end

for i=1:44;
    time(i)=t(i+1);
end

plot(time, Exergy_source, 'k', 'Linewidth', 2)
xlabel ('t (h)')
ylabel ('Xdestroyed-optical (kJ/L)')
title ('Optical Exergy Loss - 0 mM')
grid on
```

Algorithm C.25. The algorithm for CDP for the case where $[\text{NH}_4^+] = 18.7 \text{ mM}$ implemented in MATLAB programming language

M-file

```

clear all
close all

MW_biomass=23.36;
MW_tga=1023.6;

b_data=[0; 0.9; 3.97; 2955; 393.14; 11.32;628.15; 40541.751;
2577.5];

[t,x] = ode45('odetotalkinetics_first', [0 14], [0.1
0.00000001]);

for i=1:60;
    n_lipid(i,:)=((x(i+1,2)-x(i,2))/MW_tga);
    CDPlipid=cumsum(((n_lipid*b_data(8,:))/(n_lipid*11.5*b_data(4
, :)+n_lipid*21.5*b_data(3,:))));
end

for i=1:60;
    n_biomass(i,:)=((x(i+1,1)-x(i,1))/MW_biomass);
    CDPbiomass=cumsum((n_biomass*b_data(7,:))/(Nb_CO2_BP+Nb_water
_BP+Nb_nh_
_BP+Nb_hpo_BP+Nb_photon));
end

for i=1:60;
    time(i)=t(i+1);
end

[ax, h1, h2]=plotyy(time, CDPbiomass, time, CDPlipid, 'plot')

set(ax, 'xlim', [0 14], 'xtick', [0:1:14])
set(get(ax(2), 'Ylabel'), 'String', 'CDP of lipid production')
set(get(ax(1), 'Ylabel'), 'String', 'CDP of biomass production')

```

```

xlabel ('time (h)')
title ('CDP - 18.7 mM')
set(ax(2), 'ylim', [0 15], 'ytick', [0:3:15], 'ycolor', 'black');
set(ax(1), 'ylim', [0 0.6], 'ytick', [0:0.12:0.6], 'ycolor', 'black');
set(h1, 'LineStyle', '-.', 'color', 'black', 'LineWidth', 2);
set(h2, 'LineStyle', ':', 'color', 'black', 'LineWidth', 2);
legend(h1, 'CDPbiomass', 'location', 'southeast');
legend(h2, 'CDPlipid', 'location', 'southeast');
grid on

```

Algorithm C.26. The algorithm for CDP for the case where $[\text{NH}_4^+] = 6.2 \text{ mM}$ implemented in MATLAB programming language

```

M-file
clear all
close all

MW_biomass=23.36;
MW_tga=1023.6;

b_data=[0; 0.9; 3.97; 2955; 393.14; 11.32;628.15; 40541.751;
2577.5];

[t,x] = ode45('odetotalkinetics_second', [0 10], [0.25
0.00000001]);

for i=1:60;
    n_lipid(i,:)=((x(i+1,2)-x(i,2))/MW_tga);
    CDPlipid=cumsum(((n_lipid*b_data(8,:))/(n_lipid*11.5*b_data(4
, :)+n_lipid*21.5*b_data(3,:))));
end

for i=1:60;
    n_biomass(i,:)=((x(i+1,1)-x(i,1))/MW_biomass);
    CDPbiomass=cumsum((n_biomass*b_data(7,:))/(Nb_CO2_BP+Nb_water
_BP+Nb_nh_
BP+Nb_hpo_BP+Nb_photon));
end

```

```

for i=1:60;
    time(i)=t(i+1);
end

[ax, h1, h2]=plotyy(time, CDPbiomass, time, CDPlipid, 'plot')

set(ax, 'xlim', [0 10], 'xtick', [0:1:10])
set(get(ax(2), 'Ylabel'), 'String', 'CDP of lipid production')
set(get(ax(1), 'Ylabel'), 'String', 'CDP of biomass production')
xlabel ('time (h)')
title ('CDP - 6.2 mM')
set(h1, 'LineStyle', '-.', 'color', 'black', 'LineWidth', 2);
set(h2, 'LineStyle', ':', 'color', 'black', 'LineWidth', 2);
legend(h1, 'CDPbiomass', 'location', 'southeast');
legend(h2, 'CDPlipid', 'location', 'southeast');
grid on

```

Algorithm C.27. The algorithm for CDP for the case where $[\text{NH}_4^+] = 0.7 \text{ mM}$ implemented in MATLAB programming language

M-file

```

clear all
close all

MW_biomass=23.36;
MW_tga=1023.6;

b_data=[0; 0.9; 3.97; 2955; 393.14; 11.32; 628.15; 40541.751;
2577.5];

[t,x] = ode45('odetotalkinetics_third', [0 14], [0.01 0.00004]);

for i=1:68;
    n_lipid(i, :)=(x(i+1,2)-x(i,2))/MW_tga;
    CDPlipid=cumsum(((n_lipid*b_data(8, :))/(n_lipid*11.5*b_data(4, :)+n_lipid*21.5*b_data(3, :))));
end

```

```

for i=1:68;
    n_biomass(i,:)=((x(i+1,1)-x(i,1))/MW_biomass);
    CDPbiomass=cumsum((n_biomass*b_data(7,:))/(Nb_CO2_BP+Nb_water
    _BP+Nb_nh_
    BP+Nb_hpo_BP+Nb_photon));
end

for i=1:68;
    time(i)=t(i+1);
end

[ax, h1, h2]=plotyy(time, CDPbiomass, time, CDPlipid, 'plot')

set(ax, 'xlim', [0 14], 'xtick', [0:1:14])
set(get(ax(2), 'Ylabel'), 'String', 'CDP of lipid production')
set(get(ax(1), 'Ylabel'), 'String', 'CDP of biomass production')
xlabel ('time (h)')
title ('CDP - 0.7 mM')
set(h1, 'LineStyle', '-.', 'color', 'black', 'LineWidth', 2);
set(h2, 'LineStyle', ':', 'color', 'black', 'LineWidth', 2);
legend(h1, 'CDPbiomass', 'location', 'southeast');
legend(h2, 'CDPlipid', 'location', 'southeast');
grid on

```

Algorithm C.28. The algorithm for CDP for the case where $[\text{NH}_4^+] = 0$ mM implemented in MATLAB programming language

M-file

```

clear all
close all

MW_biomass=23.36;
MW_tga=1023.6;

b_data=[0; 0.9; 3.97; 2955; 393.14; 11.32; 628.15; 40541.751;
2577.5];

```



```

[t,x] = ode45('odetotalkinetics_fourth', [5 14], [0.8 0.0096]);

for i=1:44;
    n_lipid(i,:)=(x(i+1,2)-x(i,2))/MW_tga);
    CDPlipid=cumsum(((n_lipid*b_data(8,:)/(n_lipid*11.5*b_data(4
    ,:)+n_lipid*21.5*b_data(3,:)))));
end

for i=1:44;
    n_biomass(i,:)=(x(i+1,1)-x(i,1))/MW_biomass);
    CDPbiomass=cumsum((n_biomass*b_data(7,:))/(Nb_CO2_BP+Nb_water
    _BP+Nb_nh_
    BP+Nb_hpo_BP+Nb_photon));
end

for i=1:44;
    time(i)=t(i+1);
end

[ax, h1, h2]=plotxy(time, CDPbiomass, time, CDPlipid, 'plot')

set(ax, 'xlim', [5 14], 'xtick', [5:1:14])
set(get(ax(2), 'Ylabel'), 'String', 'CDP of lipid production')
set(get(ax(1), 'Ylabel'), 'String', 'CDP of biomass production')
xlabel ('time (h)')
title ('CDP - 0 mM')
set(ax(1), 'ylim', [0 40], 'ytick', [0:10:40], 'ycolor', 'black');
set(ax(2), 'ylim', [0 0.6], 'ytick', [0:0.15:0.6], 'ycolor', 'black');
set(h1, 'LineStyle', '-.', 'color', 'black', 'LineWidth', 2);
set(h2, 'LineStyle', ':', 'color', 'black', 'LineWidth', 2);
legend(h1, 'CDPbiomass', 'location', 'southeast');
legend(h2, 'CDPlipid', 'location', 'southeast');
grid on

```